Research Article

Journal of Applied Toxicology

Received: 15 September 2014, Revised: 16 October 2014, Accepted: 31 October 2014 Published online in Wiley Online Library: 22 December 2014

(wileyonlinelibrary.com) DOI 10.1002/jat.3096

Tl(I) and Tl(III) alter the expression of EGF-dependent signals and cyclins required for pheochromocytoma (PC12) cell-cycle resumption and progression

María T. L. Pino and Sandra V. Verstraeten*

ABSTRACT: The effects of thallium [Tl(I) and Tl(III)] on the PC12 cell cycle were evaluated without (EGF^-) or with (EGF^+) media supplementation with epidermal growth factor (EGF). The following markers of cell-cycle phases were analyzed: cyclin D1 (G_1); E2F-1, cyclin E and cytosolic p21 ($G_1 \rightarrow S$ transition); nuclear PCNA and cyclin A (S); and cyclin B1 (G_2). The amount of cells in each phase and the activation of the signaling cascade triggered by EGF were also analyzed. Tl(I) and Tl(III) (5–100 μM) caused dissimilar effects on PC12 cell proliferation. In EGF^- cells, Tl(I) increased the expression of $G_1 \rightarrow S$ transition markers and nuclear PCNA, without affecting cyclin A or cyclin B1. In addition to those, cyclin B1 was also increased in EGF^+ cells. In EGF^- cells, Tl(III) increased the expression of cyclin D1, all the G1→S and S phase markers and cyclin B1. In EGF^+ cells, Tl (III) increased cyclin D1 expression and decreased all the markers of $G_1 \rightarrow S$ transition and the S phase. Even when these cations did not induce the activation of EGF receptor (EGFR) in EGF^- cells, they promoted the phosphorylation of ERK1/2 and Akt. In the presence of EGF, the cations anticipated EGFR phosphorylation without affecting the kinetics of EGF-dependent ERK1/2 and Akt phosphorylation. Altogether, results indicate that Tl(I) promoted cell proliferation in both EGF^- and EGF^+ cells. In contrast, Tl(III) promoted the proliferation of EGF^- cells but delayed it in EGF^+ cells, which may be related to the toxic effects of this cation in PC12 cells. Copyright © 2014 John Wiley & Sons, Ltd.

Additional supporting information may be found in the online version of this article at the publisher's web-site.

Keywords: thallium; epidermal growth factor; cell cycle; cyclins; cell signaling

Introduction

The heavy metal thallium (Tl) is a normal component of the Earth's crust. The bioavailability of this metal is usually negligible as it forms salts and minerals that are poorly absorbed by plants and animals. Nevertheless, as a consequence of Tl mobilization by mining and its increasing use in diverse industrial activities, the air, water and soils became enriched in Tl (ATSDR, 1999; Cheam, 2001; Law and Turner, 2011). Additionally, the soils of certain regions of the world are naturally enriched in Tl (Cvjetko *et al.,* 2010), and the edible plants from those areas concentrate the metal in their roots and leaves (Wierzbicka *et al.,* 2004; Xiao *et al.,* 2004; Pavlickova *et al.,* 2006; Queirolo *et al.,* 2009). Hence, Tl is incorporated in the food chain and becomes available to humans (Bunzl *et al.,* 2001; Heim *et al.,* 2002).

The most frequent routes of human intoxication with Tl are the ingestion of or the dermal contact with Tl-containing compounds, and the inhalation of air-borne particles or fumes (Repetto *et al.,* 1998; Peter and Viraraghavan, 2005). This metal has two oxidation states, the monovalent (Tl(I)) and trivalent (Tl (III)) cations, the latter being a strong oxidant (Tl(III)/Tl(I) ε^0: +1.25 V). As a consequence, Tl(III) can oxidize certain macromolecules and alter their biological functions. In contrast, the strong oxidant environment necessary to oxidize Tl(I) to Tl(III) cannot be achieved in the intracellular milieu. Although, it has been proposed that certain plants might oxidize Tl(I) to Tl(III) (Krasnodebska-Ostrega *et al.,* 2012).

Tl is considered a cumulative poison. In rats, ^{201}Tl(I) and ^{201}Tl (III) show a similar pattern of distribution, being the kidneys the organs that accumulate the highest amounts of Tl, followed by the liver, testis and the nervous system (Sabbioni *et al.,* 1981). Accordingly, the main symptoms of chronic exposure to Tl(I) include manifestations of cardiac, renal, gastrointestinal and nervous systems dysfunction (Schaub, 1996). Tl(I) induces neurodegeneration and demyelination in the central and peripheral nervous systems, which lead to sensory and motor alterations, polyneuritis and encephalopathy, among other neurological symptoms (Galvan-Arzate and Santamaria, 1998; Heim *et al.,* 2002; Cvjetko *et al.,* 2010). As Tl crosses the placental barrier, maternal exposure to Tl during early gestation has been associated with premature deliveries and a low weight in the newborns (Hoffman, 2000). In spite of knowing the clinical symptoms caused by Tl(I) accumulation, the molecular mechanisms underlying its toxicity along with those of Tl(III), are still not completely elucidated.

*Correspondence to: Dr Sandra V. Verstraeten, Departamento de Química Biológica, IQUIFIB (UBA-CONICET), Facultad de Farmacia y Bioquímica, Universidad de Buenos Aires, Junín 956, C1113AAD, Buenos Aires, Argentina. Email: verstraeten@ffyb.uba.ar

Department of Biological Chemistry, IQUIFIB (UBA-CONICET), School of Pharmacy and Biochemistry, University of Buenos Aires, Junín 956, C1113AAD, Buenos Aires, Argentina

Journal of Applied Toxicology

We have reported previously that Tl(I) and Tl(III) cause alterations in the redox state of rat pheochromocytoma (PC12) cells (Hanzel and Verstraeten, 2006), activate the mitochondrial and/or the extrinsic pathways of apoptosis (Hanzel and Verstraeten, 2009) and destabilize lysosomes (Hanzel *et al.,* 2012). PC12 cells have an embryological origin in the neural crest (Fujita *et al.,* 1989), and thus these cells are a good model for the study of the mechanisms of action of neurotoxicants, as well as the events involved in the proliferation and differentiation of neuronal precursors (Greene and Tischler, 1976; Fujita *et al.,* 1989). The stimulation of PC12 cells with epidermal growth factor (EGF) or neuron growth factor (NGF) activates the Ras → Raf → MEK → ERK1/2 signaling cascade. The difference between both growth factors resides in the magnitude and duration of the stimulation of this pathway. EGF causes a transient activation of the signaling cascade inducing cell proliferation (Henson and Gibson, 2006), whereas NGF causes its sustained activation inducing cell differentiation (Traverse *et al.,* 1992). In line with this, it has been shown that EGF stimulates the proliferation of neuronal precursor cells in the retinal neuroepithelium (Anchan *et al.,* 1991), the olfactory epithelium (Mahanthappa and Schwarting, 1993), the embryonic mesencephalon (Mytilineou *et al.,* 1992; Santa-Olalla and Covarrubias, 1995) and the adult striatum (Reynolds *et al.,* 1992). These evidences, together with the finding that the EGF receptor (EGFR) is expressed in the germinal zones of the rat brain (Seroogy *et al.,* 1995), suggest that this growth factor may be involved in the generation of neurons both in the developing and regenerating brain (Yamada *et al.,* 1997).

Considering that the capacity of damaged organs and tissues to restore their normal functions is determined by their ability to replace damaged cells with new ones, the aim of the present work was to investigate if, besides promoting their death, Tl(I) and Tl(III) could affect PC12 cell proliferation. PC12 cells are slow-proliferating cells (Greene and Tischler, 1976) that express large amounts of EGFR (Traverse *et al.,* 1994). On this basis, we selected EGF as a stimulus to induce PC12 cell proliferation. Cell growth was stopped by serum deprivation and the cell cycle was resumed using two different protocols. In the first one, the cycle was resumed by serum replenishment with no further additions (EGF^- cells). In the second approach, besides serum replenishment, the media was supplemented with EGF (EGF^+ cells). We evaluated the effects of Tl(I) and Tl(III) on cell-cycle progression in both experimental models, characterizing the expression of the cyclins and other key regulators of this process, together with the activation of the signaling cascade that leads to cell proliferation.

Materials and Methods

Chemicals

Dulbecco´s modified Eagle medium (DMEM high glucose) and Hank's balanced salt solution were purchased from Gibco BRL (Grand Island, NY, USA). Donor horse serum was from PAA Laboratories GmbH (Pasching, Germany) and fetal bovine serum (FBS) was from Natocor (Córdoba, Argentina). Thallium(I) nitrate was from Fluka (Milwaukee, WI, USA). Thallium(III) trinitrate was from Alfa Æsar (Ward Hill, MA, USA). Murine epidermal growth factor (EGF) was from Peprotech Inc. (Rocky Hill, NJ, USA). The following primary antibodies and the appropriate horseradish peroxidase- or Texas Red-conjugated secondary antibodies were from Santa Cruz Biotechnology (Santa Cruz, CA, USA): EGFR (sc-03), cyclins D1 (sc-717), A (sc-31084), B1 (sc-245) and E (sc-25303), E2F-1 (sc-22820), p21 (sc-8246) and PCNA (sc-7907). Monoclonal primary antibodies against phospho-EGFR (Tyr1068, #3777), ERK1/2 (#9102), phospho-ERK1/2 (Thr202/Tyr204, #4370), Akt (#4691) and phospho-Akt (Ser473, #4060) were from Cell Signaling Technology Inc. (Danvers, MA, USA). The enhanced chemiluminiscence system (Pierce® ECL plus) for Western immunoblot was from Thermo Scientific (Rockford, IL, USA). Complete, EDTA-free protease inhibitor and PhosStop phosphatase inhibitor cocktails were from Roche Diagnostics GmbH (Mannheim, Germany). PVDF membranes were from Bio-Rad Corp. (Hercules, CA, USA). Prolong® Gold antifade reagent was from Life Technologies (Grand Island, NY, USA). Ribonuclease A from bovine pancreas, propidium iodide (PI), Hoechst 32258, Ponceau Red (PR) and all the other reagents had the highest quality available, and were from Sigma-Aldrich (St. Louis, MO, USA).

Tl Solutions

Tl(I) and Tl(III) stock solutions were prepared as previously described (Hanzel and Verstraeten, 2006). The amounts of Tl(I) or Tl(III) used in the experiments did not affect the pH of the culture media.

Analysis of EGF Oxidation by Tl(III)

Aliquots containing 0.1 ml of an EGF solution (25 $\mu g\,ml^{-1}$ in serum-free DMEM) were incubated at 37 °C for either 30 or 60 min in the presence of 100 μM Tl(I) or Tl(III). After incubation, the structure of EGF was verified by matrix-assisted, laser desorption/ionization time-of-flight mass spectrometry (MALDI-TOF MS) at the LANAIS-PROEM protein facility (University of Buenos Aires and National Research Council).

Cell Culture and Incubations

PC12 cells were obtained from the American Type Culture Collection (ATCC, Rockville, MD, USA), and cultured in DMEM supplemented with 10% horse serum, 5% FBS, 100 units per ml of penicillin G, 100 $\mu g\,ml^{-1}$ streptomycin and 4 mM L-glutamine at 37 °C in a 5% CO_2 atmosphere (Hanzel and Verstraeten, 2006). All experiments were performed using cell cultures between passages 10 and 25.

Cells were harvested by 5-min incubation at 37 °C in the presence of sterile 0.125% (w/v) trypsin and 0.02% (w/v) disodium EDTA in Hank's balanced salt solution (pH 7.2). As indicated for the individual experiments, cells were seeded on poly-L-lysine-treated 60- or 100-mm culture dishes, and allowed to grow until ~60% of confluence. Cell growth was stopped by serum deprivation for 24 h. Next, the culture medium was replaced by complete medium without (EGF^- cells) or with (EGF^+ cells) the addition of 10 $ng\,ml^{-1}$ EGF, and with or without the simultaneous addition of Tl(I) or Tl(III) (5–100 μM). Cells were harvested at different times and processed as indicated for the individual experiments.

Cell-Cycle Analyzes

To analyze the kinetics of the PC12 cell cycle, cells were grown in the conditions described above, and EGF^- and EGF^+ cells were incubated for 3 to 48 h of cell-cycle resumption. To analyze the

effects of Tl(I) and Tl(III) on EGF^- and EGF^+ cell-cycle progression, cells were incubated for either 24 or 30 h of in the presence of Tl (I) or Tl(III) (10–100 μM). After incubation, cells were collected by scrapping, centrifuged at 800 *g* for 10 min at 4 °C, and washed twice with pre-warmed phosphate-buffered saline (PBS). Cells were suspended in 1 ml of fixation solution [70% (v/v) ethanol, 0.5% (v/v) Tween-20 in PBS], and kept at 4 °C for at least 24 h. After centrifugation at 800 *g* for 10 min at 4 °C, cells were washed twice with PBS, suspended in 0.1 ml of a solution containing 50 μM propidium iodide (PI) and 0.1 mg ml^{-1} DNAse-free ribonuclease A, and incubated at room temperature for 30 min. Samples were then filtered through a nylon mesh to disrupt cell aggregates. DNA content in the samples was evaluated in a FacsCalibur cytometer (Beckton-Dickinson, Mountain View, CA, USA), equipped with a 488-nm laser and recorded in a FL2 channel (585 nm). Acquired raw data were analyzed with the freeware software WinMDI 2.9 (http://www.cyto.purdue.edu/flowcyt/software/Winmdi.htm), and cell-cycle distribution was analyzed with the histogram deconvolution software Cylchred 1.0 (Cardiff University, Wales, UK).

Preparation of Cell Fractions for Western Blot Analysis

PC12 cells were grown on 100-mm-diameter culture dishes (1×10^7 cells), and incubated for 24 h in the conditions described above. Cells were washed twice with pre-warmed PBS, collected by scrapping, centrifuged at 800 *g* for 10 min at 4 °C, and the pellets were frozen for at least 1 h at −80 °C. Whole cell lysates were obtained (Hanzel and Verstraeten, 2009) for the detection of p-EGFR, total EGFR, p-ERK1/2, total ERK1/2, p-Akt, total Akt, cyclins D1, E, A and B1 and E2F-1. Nuclear and cytosolic fractions for the analysis of p21 and PCNA levels were obtained as described previously (Muller *et al.,* 1997). Samples were added with protease and phosphatase inhibitor cocktails to prevent protein degradation during their manipulation and storage. After protein quantification (Bradford, 1976), samples were stored at −80 °C until their use.

Western Blot Analysis

Proteins were separated by reducing SDS–PAGE electrophoresis, and transferred to PVDF membranes. Colored molecular weight standards (GE Healthcare, Piscataway, NJ, USA) were ran simultaneously. Membranes were blocked for 1 h in 5% (w/v) bovine serum albumin in PBS, incubated overnight at 4 °C in the presence of the corresponding primary antibody. The following dilutions of antibodies were used: Akt and ERK1/2 1:2,000; p-ERK1/2, cyclins D1, A and E, E2F-1, and PCNA 1:1,000; p-EGFR, EGFR, p-Akt and p21 1:500; cyclin B1 1:200. Membranes were further incubated for 90 min with the corresponding peroxidase-conjugated secondary antibody (1:10 000 dilution). Specific bands were revealed with chemiluminiscent Pierce® ECLplus Western blot substrate and detected in a Storm Phosphoimager 840 (Molecular Dynamics, Sunnyvale, CA, USA). Western blot data were quantified using a Gel-Pro Analyzer 4.0 (Media Cybernetics Inc., Bethesda, MD, USA). The integrated optical density of the bands was normalized by total protein content in the lane evaluated by Ponceau Red (PR) staining.

Immunofluorescence Detection of Cyclin D1, p21 and PCNA

PC12 cells were grown on a 18-mm-diameter glass cover slip and incubated in the conditions described above. Cyclin D1, PCNA and p21 were immunolocalized (primary antibody dilution 1:50) as described previously (Hanzel *et al.,* 2012), and detected with the corresponding Texas Red-conjugated secondary antibody (1:200 dilution). Cover slips were washed three times with PBS and mounted using Prolong® Gold antifade reagent containing Hoechst 32258 (5 μM). For the evaluation of cyclin D1 and p21 localization, cells were observed through an Olympus BX50 fluorescence microscope with a coupled digital camera (Olympus Optical Co., Ltd, Tokyo, Japan). For the evaluation of PCNA localization, cells were observed under an Olympus Fluoview FV1000 confocal microscope (Olympus Corporation, Tokyo, Japan) with objective lens USLSAPO 609 NA 1:35 and magnification 600×. The degree of colocalization of PCNA with nuclei labeling was evaluated from the changes in the overlap coefficient according to Manders *et al.* (1993) using the routines available in the software Image-Pro Plus 5.1 (Media Cybernetics Inc., Bethesda, MD, USA).

Statistical Analysis

The effects of EGF on PC12 cells were analyzed by the Student's *t*-test. The effects of Tl(I) and Tl(III) were analyzed by one-way analysis of variance (ANOVA) followed by Fisher's protected least square difference test. The comparison between the effects of Tl (I) and Tl(III) were performed by two-way ANOVA followed by Bonferroni's post-test. All statistical analyzes and correlations were performed using the routines available in GraphPad Prism version 5.00 for Windows, GraphPad Software (San Diego, CA, USA). A probability (P)-value < 0.05 was considered statistically significant.

Results

Cell Cycle Progression in PC12 Cells

To characterize the kinetics of cell cycle progression, the ploidy of PC12 (EGF^-) cells was evaluated by nuclei staining with PI, followed by the identification of the populations of cells in G_0/G_1, S or G_2/M phase by flow cytometry. Prior to the experiments, cultures were enriched in cells with G_1-phase DNA content (Cooper, 2003) by a 24-h serum deprivation. Based on their DNA content, the percentage of cells in each phase was G_0/G_1: 80 ± 1, S: 13 ± 1, and G_2/M: 6 ± 1, respectively (time 0, Fig. 1). After serum replenishment, the amount of cells in G_1 phase decreased and reached a minimum level between 18 and 24 h of incubation (Fig. 1A), which corresponded to the appearance of the S phase (Fig. 1B). The amount of cells in G_2/M phases increased gradually, although a maximum was not clearly observed within the period assessed (Fig. 1C). At prolonged incubations, cell cultures became asynchronous and they were not analyzed (data not shown).

The same analysis was performed for PC12 cells supplemented with EGF (EGF^+ cells). In these cells, the decrease in the G_0/G_1 phase was anticipated in ~9 h with respect to EGF^- cells and it was sustained until 24 h (Fig. 1A). The amount of cells in the S phase increased progressively between 6 and 24 h from cell cycle re-entry. In contrast to that observed in EGF^- cells, the amount of cells in the G_2/M phase had two maximums. The first one was observed at 9 h and corresponded to cells that at the start of the experiment were in the S phase. The second was found at 30 h post-serum replenishment and corresponded to those cells that reached the S phase within 6 and 24 h of incubation.

Journal of Applied Toxicology

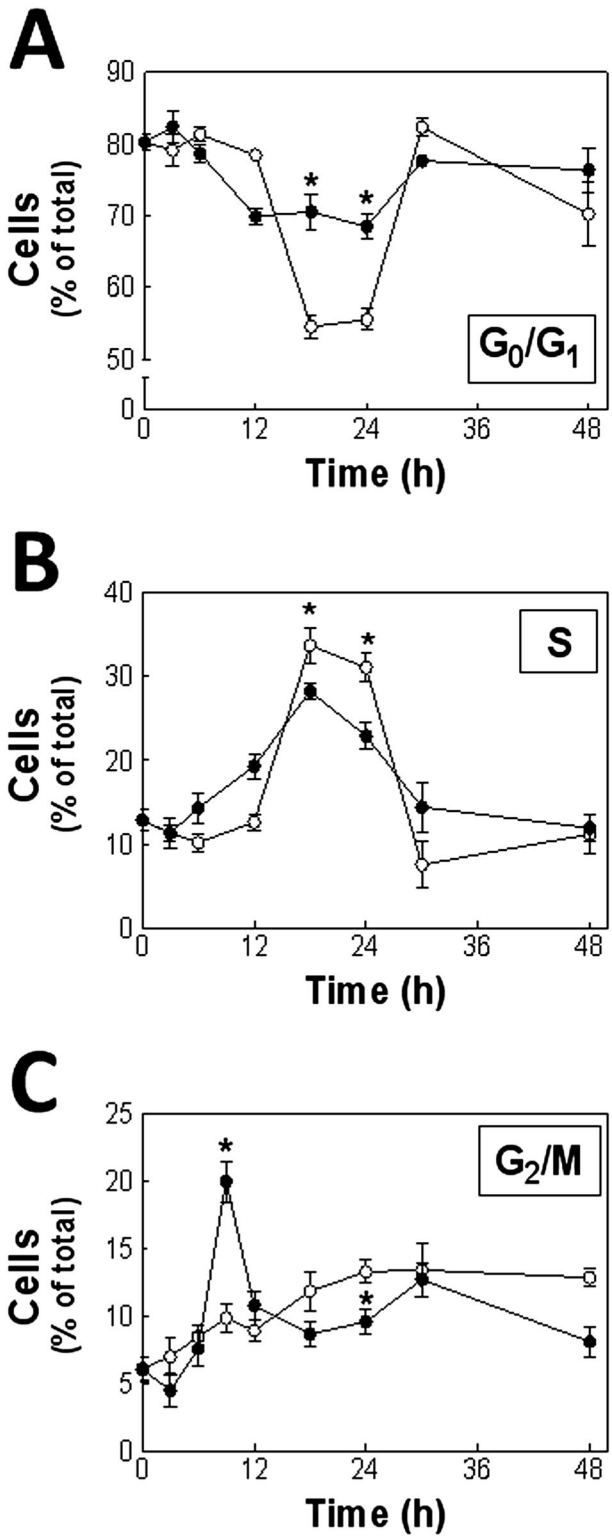

Figure 1. Evaluation of cell cycle in PC12 cells. PC12 cells were incubated at 37 °C for 24 h in serum-free Dulbecco´s modified Eagle medium (DMEM). After media replacement, the relative amount of cells in (A) G_0/G_1, (B) S and (C) the G_2/M phase of the cell cycle was measured in EGF^- (○) and EGF^+ (●) cells between 3 and 48 h of incubation. Results are expressed as the mean ± SEM of at least four independent experiments. *Significantly different from the value measured in EGF^- cells ($P < 0.001$).

Effects of Tl(I) and Tl(III) on the Progression of the Cell Cycle

For comparative purposes, the effects of Tl(I) and Tl(III) on the amount of cells in each phase of the cell cycle were evaluated at two fixed time points (24 and 30 h) after cell-cycle resumption.

After 24 h of EGF^- cell exposure to 10–50 μM Tl(I) (Fig. 2A), the amount of cells in G_0/G_1, S and G_2/M phase were similar to those found in controls. At 100 μM Tl(I), the amount of EGF^- cells in the S phase was increased by 31% and those in G_2/M decreased by 31% ($P < 0.05$ with respect to the controls). After 30 h, the amount of EGF^- cells in the S phase was still increased but only for the highest concentration of Tl(I) assessed. The amount of cells in G_2/M phase increased in a concentration (10–50 μM)-dependent manner. Tl(I) increased the amount of EGF^+ cells in the S phase both at 24 and 30 h of cell-cycle resumption (Fig. 2B). In contrast, the amount of cells in G_2/M phase was decreased at 24 h but it was normalized at 30 h of cell-cycle resumption.

The exposure of EGF^- cells to Tl(III) for 24 h resulted in a concentration-dependent decrease in the percentage of cells in S phase (Fig. 2C). This effect was significant only for the highest concentration of Tl(III) assessed (−28% respect to the controls, $P < 0.05$) and it was accompanied by increased levels of cells in G_2/M (+66% respect to controls, $P < 0.05$). In contrast, after 30 h of cell exposure to Tl(III), decreased amounts of cells in G_1 (−20% respect to the controls, $P < 0.05$) and increased amounts of cells in the S phase (+43% respect to controls, $P < 0.05$) were found. In EGF^+ cells exposed for 24 h to Tl (III) (Fig. 2D), increased amounts of cells in G_0/G_1 (+13% with respect to the controls, $P < 0.05$) and decreased amounts of cells in G_2/M (−25% with respect to the controls, $P < 0.05$) were observed. After 30 h of exposure, the amount of cells in G_0/G_1 returned to control values, although the amount of cells in the S phase decreased up to 30% at 10 μM Tl(III) ($P < 0.05$ with respect to the controls).

Effects of Tl(I) and Tl(III) on the Expression of Regulators of Cell Cycle Progression

On this basis, we next investigated if Tl may affect the expression of the cyclins that govern the different stages of the cell cycle: cyclins D1 and E (G_1 phase), cyclin A (S phase) and cyclin B1 (M phase).

After 24 h of serum replenishment, the levels of cyclin D1 in EGF^+ and EGF^- cells were similar (Fig. 3A, B). In EGF^- cells, Tl(I) showed a dual effect on cyclin D1 expression, decreasing its content in the 5–25 μM range of concentrations, and increasing it at 50 μM (Fig. 3C). Tl(III) did not alter the cyclin D1 content in these cells (Fig. 3D). In EGF^+ cells, both Tl(I) (25–100 μM) and Tl(III) (5–100 μM) significantly increased the content of cyclin D1 ($P < 0.005$) (Fig. 3C, D). The magnitude of the effect due to Tl(III) was significantly higher than that due to Tl(I) in the 10–50 μM range of concentrations ($P < 0.05$). In spite of having higher levels of cyclin D1, the immunolocalization of cyclin D1 was similar in EGF^- and EGF^+ cells treated with 100 μM Tl(I) or Tl(III) (Figure 3E). At this concentration of Tl, the levels of cyclin D1 expression found in EGF^+ cells correlated positively ($P < 0.001$) with the relative amount of cells in the G_0/G_1 phase (Fig. 3F).

The content of the transcription factor E2F-1 in EGF^+ cells was 80% higher than that found in EGF^- cells ($P < 0.001$) (Fig. 4A, B). In EGF^- cells, both Tl(I) and Tl(III) increased E2F-1 expression (Fig. 4C, D) although the magnitude of the effect

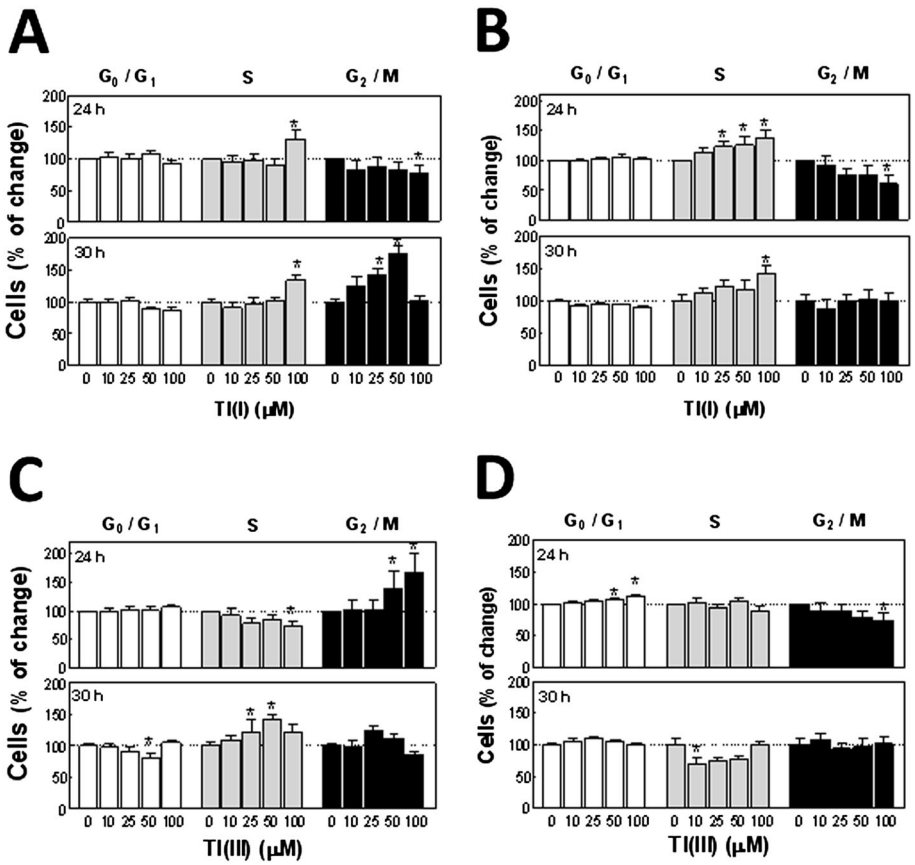

Figure 2. Effects of Tl on PC12 cell-cycle progression. PC12 cells were incubated at 37 °C for 24 h in serum-free Dulbecco´s modified Eagle medium (DMEM). After media replacement, EGF^- (A, C) and EGF^+ (B, D) cells were incubated for a further 24 or 30 h in the presence of 10–100 μM Tl(I) (A, B) or Tl(III) (C, D). The amount of cells in each phase of the cycle was quantified by nuclear staining with PI and flow cytometry. Results are expressed as the percentage of cells in each phase with respect to the value measured in the control cells, and are shown as the mean ± SEM of at least four independent experiments. *Significantly different from the value measured in cells incubated in the absence of Tl ($P < 0.01$).

due to Tl(I) was higher than that due to Tl(III). In EGF^+ cells, Tl (I) (25–50 μM) increased the E2F-1 content whereas Tl(III) (5–50 μM) decreased it ($P < 0.01$; Fig. 4C, D). Although, at the 100 μM concentration, Tl(III) increased E2F-1 content by 25% ($P < 0.05$ with respect to the controls). Basal cyclin E levels were 51% higher in EGF^+ with respect to EGF^- cells ($P < 0.005$; Fig. 5A, B). In EGF^- cells, Tl(I) (50–100 μM, Fig. 5C) and Tl(III) (25–100 μM, Fig. 5D) significantly increased cyclin E contents ($P < 0.01$ with respect to the controls). In EGF^+ cells, 100 μM Tl(I) and Tl(III) significantly increased cyclin E expression ($P < 0.01$ with respect to the controls) (Fig. 5C and D).

Next, we investigated if the higher expression levels of cyclins D1 and E found in Tl(I)- and Tl(III) (50–100 μM)-treated cells were accompanied by the translocation of p21 (from the nuclei to the cytosol) and PCNA (from the cytosol to the nuclei). For this, the relative amounts of these two proteins in nuclear and cytosolic fractions were measured. The basal cytosolic to nuclear p21 ratio was significantly higher in EGF^+ than in the EGF^- cells (+51%, $P < 0.01$) (Fig. 6A and B). Both in EGF^- and EGF^+ cells, Tl(I) and Tl(III) (50–100 μM) significantly promoted p21 translocation to the cytosol ($P < 0.01$ with respect to the controls), with a magnitude that ranged from 80% to 210% increase with respect to the data measured in their respective controls (Fig. 6C, D). Supporting these results a strong nuclear immunolocalization of p21 was evidenced in EGF^- cells (Fig. 6E). At a 100-μM concentration, Tl(I) and to a lesser extent Tl(III), caused p21 translocation to cytoplasm. In EGF^+ cells, p21 was localized mostly in the cytoplasm both before and after cell exposure to 100 μM Tl(I) or Tl(III) (Fig. 6E).

The basal nuclear to cytoplasmic PCNA ratio in EGF^+ cells was 3.4-times higher than the value measured in EGF^- cells ($P < 0.001$) (Fig. 7A, B). In EGF^- cells, both Tl(I) and Tl(III) (50–100 μM) increased the nuclear to cytosolic PCNA ratio (Fig. 7C and D), in a magnitude that was significant ($P < 0.01$ with respect to the controls) for 50 μM Tl(I) and 100 μM Tl(III). In EGF^+ cells, Tl(I) and Tl(III) had opposed effects. While Tl(I) significantly increased ($P < 0.01$ with respect to the controls) the content of nuclear PCNA, Tl(III) decreased it ($P < 0.01$ with respect to the controls) (Fig. 7C, D). These results were confirmed by immunofluorescence detection of PCNA, showing higher PCNA colocalization with nuclear staining in EGF^- cells exposed to 100 μM Tl(I) or Tl(III) than the control cells (Fig. 7E). In EGF^+ cells, Tl(I) increased PCNA nuclear localization whereas Tl(III) mildly decreased it (Fig. 7E). The nuclear-to-cytosolic PCNA ratio measured in 100 μM Tl-treated cells significantly correlated with the calculated overlapping coefficients for both EGF^- (r^2: 0.99, $P < 0.01$) and EGF^+ (r^2: 0.99, $P < 0.05$) cells (Fig. 7F).

The total content of cyclin A in EGF^+ cells was 2.5-times higher with respect to that measured in EGF^- cells ($P < 0.01$) (Fig. 8A, B). The ratio between the inactive (48 kDa) and active (55 kDa) forms of cyclin A was significantly lower in EGF^+ cells with respect to EGF^- cells ($P < 0.01$) (Fig. 8B). Tl(I) did not affect the total

Journal of AppliedToxicology

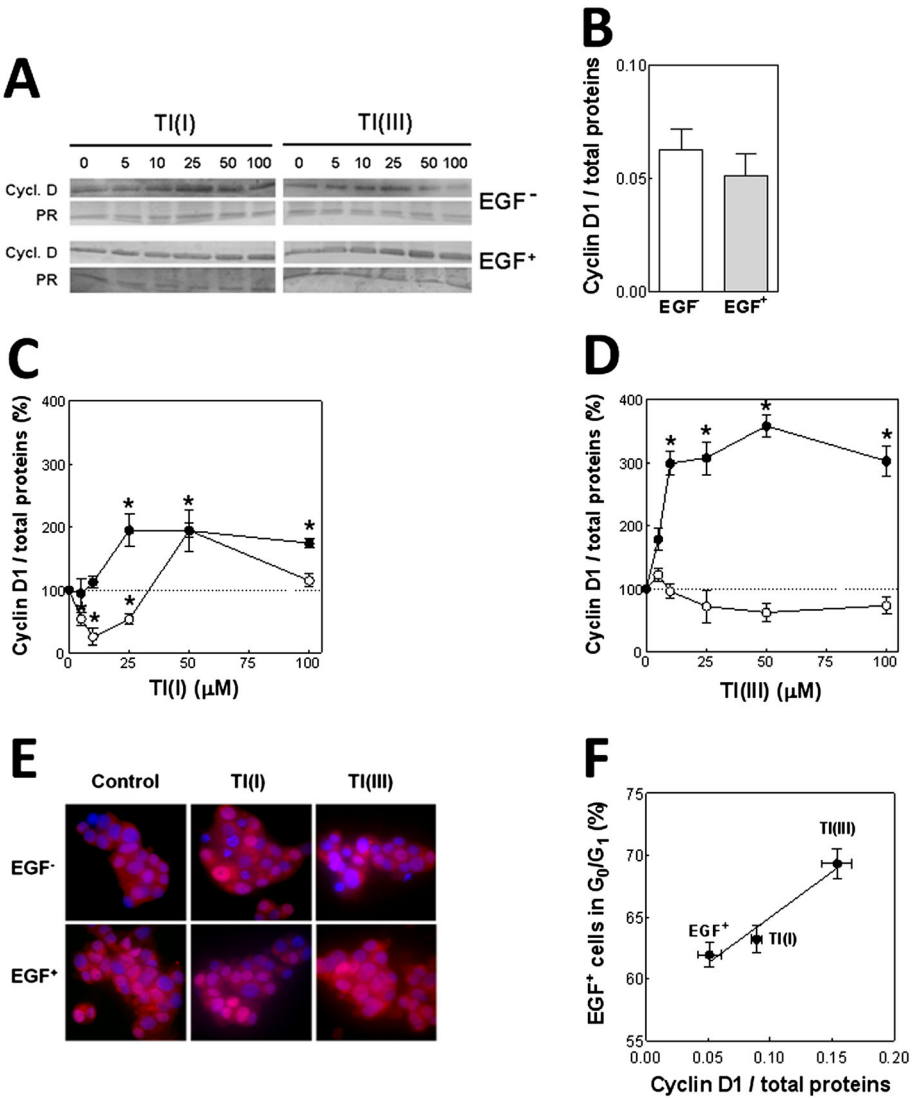

Figure 3. Effects of Tl on cyclin D1 expression. PC12 cells were incubated at 37 °C for 24 h in serum-free Dulbecco´s modified Eagle medium (DMEM). After media replacement, EGF^- and EGF^+ cells were incubated for a further 24 h in the presence of 5–100 μM Tl(I) or Tl(III), and cyclin D1 expression was evaluated. (A) Representative Western blots. Loading control was performed by Ponceau Red (PR) protein staining and the region of the membrane corresponding to cyclin D1 (34 kDa) migration is shown. (B–D) Relative cyclin D1 content in EGF^- (○) and EGF^+ (●) cells (B), and in Tl(I)- (C) or Tl(III)-treated cells (D). * Significantly different from the value measured in cells incubated in the absence of Tl ($P < 0.01$). (E) Immunolocalization of cyclin D1 in EGF^- and EGF^+ cells exposed for 24 h to 100 μM Tl(I) or Tl(III) and visualized by fluorescence microscopy. *Red*: cyclin D1; *blue*: nuclei. (F) Correlation between the amount of cells in G_0/G_1 phase in EGF^+ cells incubated for 24 h in the absence of Tl (EGF^+) or in the presence of 100 μM Tl(I) or Tl(III) and the expression levels of cyclin D1.

content of cyclin A in EGF^- or EGF^+ cells (Fig. 8C). In contrast, Tl (III) had opposed effects on EGF^- and EGF^+ cells. While in EGF^- cells treated with Tl(III) total cyclin A levels were not affected, in EGF^+ cells Tl(III) decreased cyclin A levels by 38–70% ($P < 0.001$ with respect to the controls) (Fig. 8D). Tl(I) increased the ratio between the inactive and active forms of cyclin A in both EGF^- and EGF^+ cells (Fig. 8E), whereas Tl(III) increased this ratio only in the EGF^- cells (Fig. 8F).

Finally, basal cyclin B1 levels were similar in EGF^- and EGF^+ cells (Fig. 9A, B). In EGF^- cells, Tl(I) (100 μM) and Tl(III) (10–50 μM) significantly increased cyclin B1 levels ($P < 0.01$ with respect to the controls) (Fig. 9C, D). In EGF^+ cells, Tl(I) (10–50 μM) significantly increased cyclin B1 levels ($P < 0.01$ with respect to the controls) whereas Tl(III) did not affect cyclin B1 levels in the range of concentrations assessed (Fig. 9C, D)

Effects of Tl(I) and Tl(III) on EGFR-Dependent Signaling Cascade

To understand further the mechanisms underlying the alteration of cyclins expression in cells exposed to Tl(I) or Tl(III), the signaling cascade activated by EGF was evaluated both in EGF^- and EGF^+ cells. Measurements were restricted to the maximal concentration of Tl assessed (100 μM) as this concentration altered almost every parameter evaluated in this study.

Tl(III) is a strong oxidant and the possibility that it may oxidize EGF was evaluated in a cell-free system. For that purpose, EGF was incubated in the presence of 100 μM Tl(III), and the generation of oxidized species of EGF were analyzed by MALDI-TOF MS. Using this method, oxidized EGF should be evidenced as a peak with *m/z* +16 corresponding to the

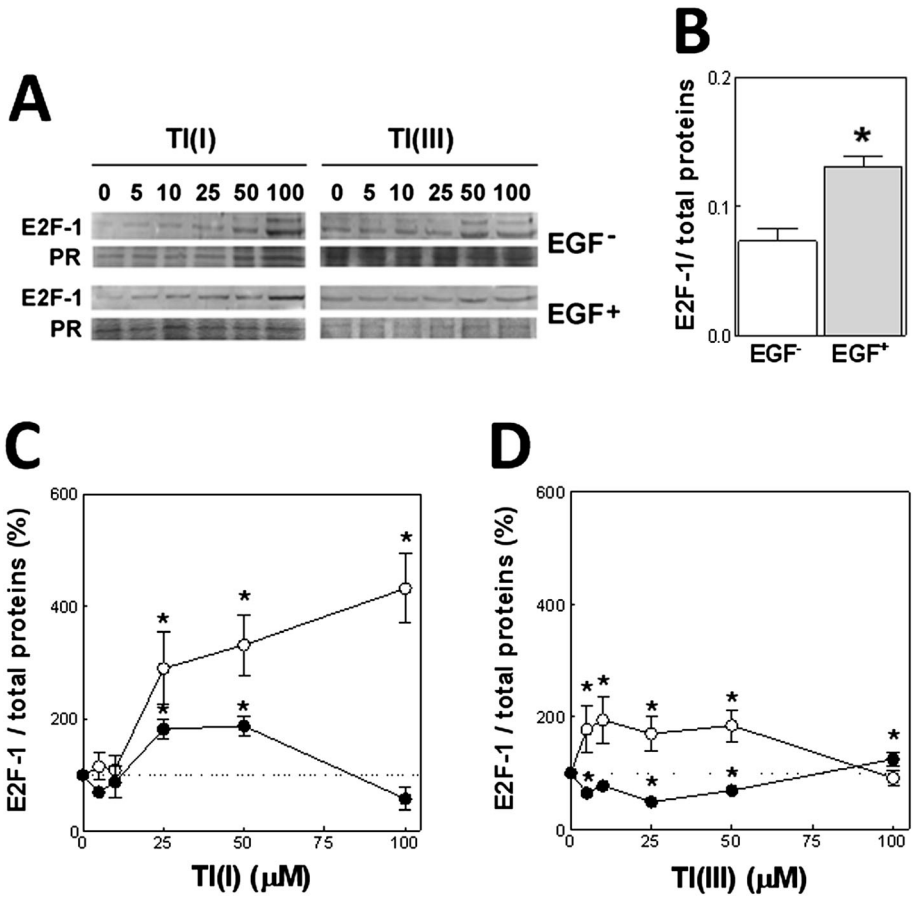

Figure 4. Effects of Tl on E2F-1 expression. PC12 cells were incubated at 37 °C for 24 h in serum-free Dulbecco´s modified Eagle medium (DMEM). After media replacement, EGF^- and EGF^+ cells were incubated for a further 24 h in the presence of 5–100 μM Tl(I) or Tl(III), and E2F-1 expression was evaluated. (A) Representative Western blots. Loading control was performed by Ponceau Red (PR) protein staining and the region of the membrane corresponding to E2F-1 (60 kDa) migration is shown. Graphs show the relative E2F-1 content in EGF^- (○) and EGF^+ (●) cells (B), and in Tl(I)- (C) or Tl (III)-treated cells (D). Results are shown as the mean ± SEM of at least four independent experiments. *Significantly different from the value measured in cells incubated in the absence of Tl ($P < 0.01$).

oxidation of Met_{21}, Trp_{49} or Trp_{50}. The similarities between the spectrum corresponding to EGF alone (Supplementary Figure 1A) and those obtained for EGF incubated in the presence of Tl(III) for either 30 min (Supplementary Figure S1B) or 60 min (Supplementary Figure S1C) suggest that Tl(III) did not cause the irreversible oxidation of EGF. As expected from its lack of oxidant capacity, Tl(I) did not affect EGF mass spectrum (data not shown).

Once discarded the possibility that Tl(III) could alter the molecular integrity of EGF and thus decrease the effective concentration of EGF available to initiate the signaling cascade, the kinetics of EGF receptor (EGFR) activation was evaluated by its degree of phosphorylation (Fig. 10A). In EGF^- cells, the phosphorylation of EGFR increased slightly over the 90-min period assessed (Fig. 10B). As expected, the content of p-EGFR in EGF^+ cells was significantly higher than in EGF^- cells ($P < 0.01$) with a maximum attained after 10 min of EGF addition to the media (Fig. 10A, B). In EGF^- cells, Tl(I) and Tl(III) did not affect the kinetics of EGFR phosphorylation (Fig. 10C). In contrast, both Tl(I) and Tl (III) stimulated EGFR phosphorylation in EGF^+ cells ($P < 0.001$ with respect to the controls) between 1 and 5 min after EGF addition to the samples (Fig. 10D). At prolonged times, the phosphorylation of EGFR in Tl(I)- and Tl(III)-treated EGF^+ cells was similar to that measured in EGF^+ cells without the addition of Tl (Fig. 10D).

The phosphorylation of ERK1/2 that occurs downstream of EGFR activation was next evaluated (Fig. 11A). EGF^+ cells showed significantly higher contents of p-ERK1 and p-ERK2 than EGF^- cells ($P < 0.01$), with a maximum reached after 5 min of EGF addition to the media (Fig. 11B). At prolonged incubation times, the magnitude of ERK1 and ERK2 phosphorylation was similar in EGF^- and EGF^+ cells (Fig. 11A and B). In EGF^- cells, Tl(I) and Tl(III) stimulated ERK1 and ERK2 phosphorylation (Fig. 11D and F) between 5 and 10 min of incubation ($P < 0.005$ with respect to the controls) returning to baseline values at prolonged incubations. In EGF^+ cells, the levels of p-ERK1 in Tl(I)- or Tl(III)-treated cells were maximal between 1 and 5 min of incubation ($P < 0.01$ with respect to the controls), whereas at prolonged incubation times p-ERK1 levels were similar to that found in cells devoid Tl (Fig. 11D). The kinetics of ERK2 phosphorylation in EGF^+ cells was not affected by Tl(I) or Tl(III) along the period assessed (Fig. 11G).

Finally, the activation of Akt was investigated (Fig. 12A). EGF^+ cells showed significantly higher contents of p-Akt than EGF^- cells ($P < 0.01$), with a maximum attained after 5 min of EGF addition to the media, and that decreased progressively until reaching values similar to those found in EGF^- cells (Fig. 12B). Between 1 and 10 min, EGF^- cells treated with Tl(I) showed a tendency towards increased Akt phosphorylation, both Tl(I)

Journal of Applied Toxicology

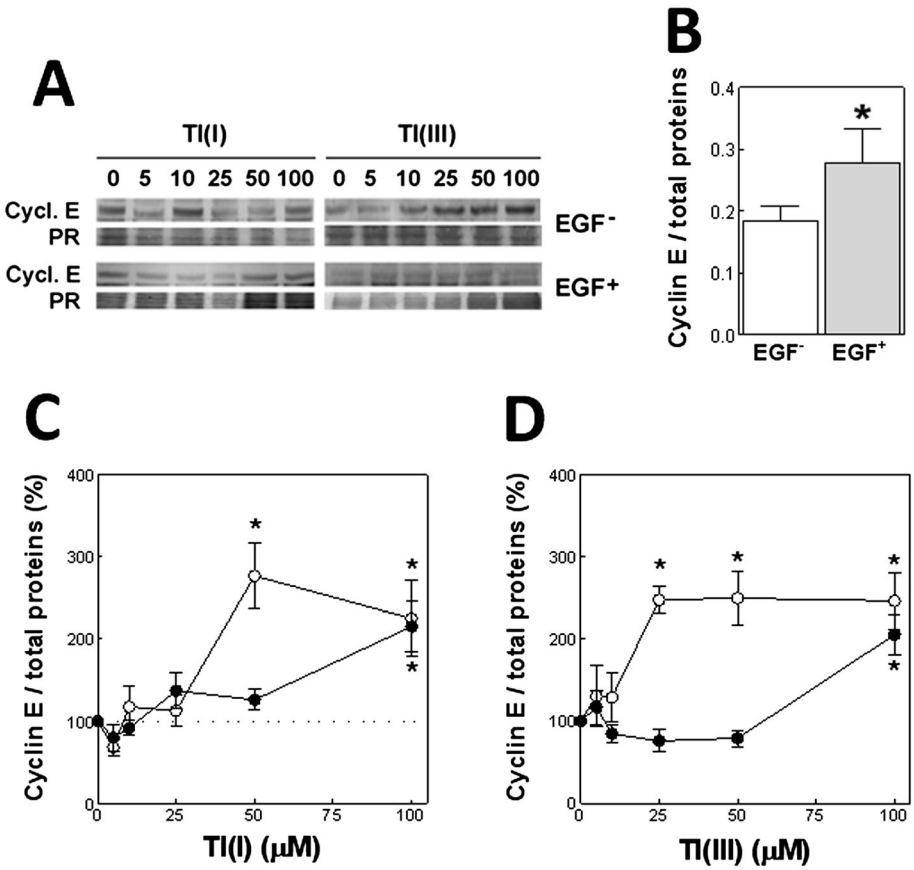

Figure 5. Effects of Tl on cyclin E expression. PC12 cells were incubated at 37 °C for 24 h in serum-free Dulbecco´s modified Eagle medium (DMEM). After media replacement, EGF^- and EGF^+ cells were incubated for a further 24 h in the presence of 5–100 μM Tl(I) or Tl(III), and cyclin E expression was evaluated. (A) Representative Western blots. Loading control was performed by Ponceau Red (PR) protein staining and the region of the membrane corresponding to cyclin E (53 kDa) migration is shown. Graphs show the relative cyclin E content in EGF^- (○) and EGF^+ (●) cells (B), and in Tl (I)- (C) or Tl(III)-treated cells (D). Results are shown as the mean ± SEM of at least four independent experiments. * Significantly different from the value measured in cells incubated in the absence of Tl ($P < 0.01$).

and Tl(III) increased Akt phosphorylation in EGF^- cells, being the magnitude of Tl(III)-mediated effect higher than that of Tl(I) (Fig. 12C). In EGF^+ cells, Tl(I) and Tl(III) did not affect EGF-dependent Akt phosphorylation between 1 and 10 min of EGF addition. However, after 15 min of EGF addition, p-Akt levels remained elevated in Tl(III)-treated cells ($P < 0.01$ with respect to the controls) (Fig. 12D). Akt phosphorylation measured after 15 min of EGF^+ cells exposure to Tl significantly correlated with the expression levels of cyclin D1 (r^2: 0.93, $P < 0.05$; Fig. 12E) and with the amount of cells in the G_0/G_1 phase of the cycle measured after 24 h (r^2: 0.95, $P < 0.05$; Fig. 12F).

Discussion

Tissues and organs homeostasis results from the balance between the disappearance of aged or damaged cells and the generation of new ones. For that reason, the maintenance of the machinery that regulates cell proliferation is a key event in determining the organogenesis and development.

The exposure of cells to toxic heavy metals may interfere with the progression of the cell cycle and/or to promote cell death. For example, high doses of cadmium, cobalt, lead or mercury induce the arrest of the cell cycle in diverse experimental models (Gastaldo *et al.,* 2007; Glahn *et al.,* 2008; Bose *et al.,* 2012; Darolles *et al.,* 2013; Smith *et al.,* 2014), whereas at low doses, cadmium induces cell proliferation (Ronchetti *et al.,* 2013; Zhou *et al.,* 2013; Simoniello *et al.,* 2014). Akin to cadmium, lead and mercury, Tl is considered as a priority pollutant by the USA Environmental Protection Agency. In addition to causing cell death in diverse experimental models, Tl(I) caused DNA alterations in bacteria, plants and cultured mammalian cells (Rodriguez-Mercado and Altamirano-Lozano, 2013). Moreover, a pilot study suggested that Tl(I)-poisoned patients have an increased frequency of structural chromosomal aberrations compatible with those caused by S-dependent clastogens (Nikiforov *et al.,* 1999).

The present study was started to characterize the kinetics of the PC12 cell cycle. Samples were enriched in cells with G_1-amounts of DNA by 24-h serum deprivation (Cooper, 2003). Then, the cycle was resumed replenishing the serum in the media either without or with the addition of EGF (10 ng ml^{-1}). Even when the complete culture media used for the experiments contained 10% horse and 5% FBS, it caused minimal EGFR activation. EGFR has two specific binding sites, one that binds EGF with high affinity [dissociation constant (Kd) < 1 nM] and the other that binds EGF with low affinity (Kd = 6–12 nM) (Suresh Babu *et al.,* 2004). Given that the estimated concentration of EGF in the culture media [5–18 pM, (Joh *et al.,* 1986; Hwang *et al.,* 1989; Birk *et al.,* 1999)] was at least two orders of magnitude lower than that required to stimulate the high-affinity binding sites of EGFR,

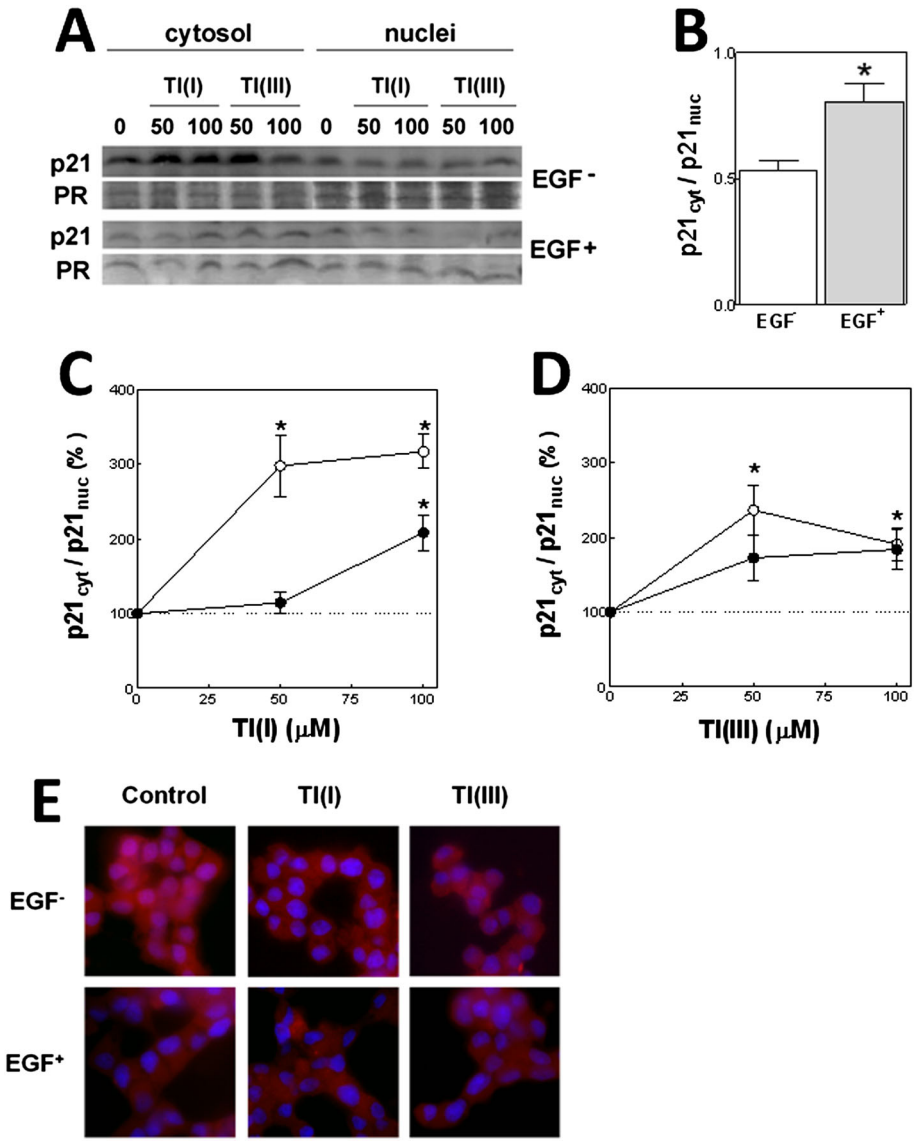

Figure 6. Effects of Tl on p21 localization. PC12 cells were incubated at 37 °C for 24 h in serum-free Dulbecco´s modified Eagle medium (DMEM). After media replacement, EGF^- and EGF^+ cells were incubated for a further 24 h in the presence of 50 or 100 μM Tl(I) or Tl(III), and p21 expression was evaluated in cytosol and nuclear fractions. (A) Representative Western blots. Loading control was performed by Ponceau Red (PR) protein staining and the region of the membrane corresponding to p21 (21 kDa) migration is shown. Graphs show the relative p21 content in cytosol ($p21_{cyt}$) and nuclear ($p21_{nuc}$) fractions in EGF^- (○) and EGF^+ (●) cells (B), and in Tl(I)- (C) or Tl(III)-treated cells (D). Results are shown as the mean ± SEM of three independent experiments. * Significantly different from the value measured in cells incubated in the absence of Tl ($P < 0.01$). (E) Immunolocalization of p21 in EGF^- and EGF^+ cells exposed for 24 h to 100 μM Tl(I) or Tl(III) and visualized by fluorescence microscopy. *Red*: p21; *blue*: nuclei.

negligible activation of this receptor can be expected in EGF^- cells. Supporting that, when the culture media was supplemented with 10 ng ml^{-1} (1.65 nM) EGF, a concentration close to the Kd of EGFR high-affinity binding sites, the phosphorylation of EGFR increased 12 times in the first 10 min of incubation. Because of the large amount of EGFR expressed in this cell line (Traverse *et al.,* 1994), the maximal EGFR activation was not achieved in the current conditions (Suresh Babu *et al.,* 2004).

The kinetics of PC12 cells cycle was evaluated between 3 and 48 h after cell-cycle resumption. It has been reported that maximal [^{3}H]thymidine incorporation occurs in these cells between 18 and 20 h after resuming the cycle (Rudkin *et al.,* 1989), with a doubling time estimated in 40 h (Mouri and Sako, 2013). In our model, the maximal percentage of cells in the S phase was observed between 18 and 24 h after the cycle resumption. In accordance to Lee and Lo (2010), only ~30% of EGF^- cells reached the S phase, whereas 60% of them remained in G_1 phase. In EGF^+ cells, the onset of the S phase was anticipated in ~9 h with respect to that in EGF^- cells and persisted until 24 h of cell-cycle resumption. Even when the lengths of the S phase in EGF^- and EGF^+ cells were different, data integration of the curves depicted in Fig. 1B indicated that the total amount of cells that reached the S phase was similar for both experimental conditions (EGF^- cells: 33%, EGF^+ cells: 28%). The anticipation of cell entry in S phase caused by EGF is consistent with the continuum model of the mammalian cell division cycle (Cooper 2000, 2003).

Next, the effects of Tl(I) and Tl(III) (5–100 μM) on the PC12 cell cycle were evaluated. The range of Tl concentrations (5–100 μM)

Journal of Applied Toxicology

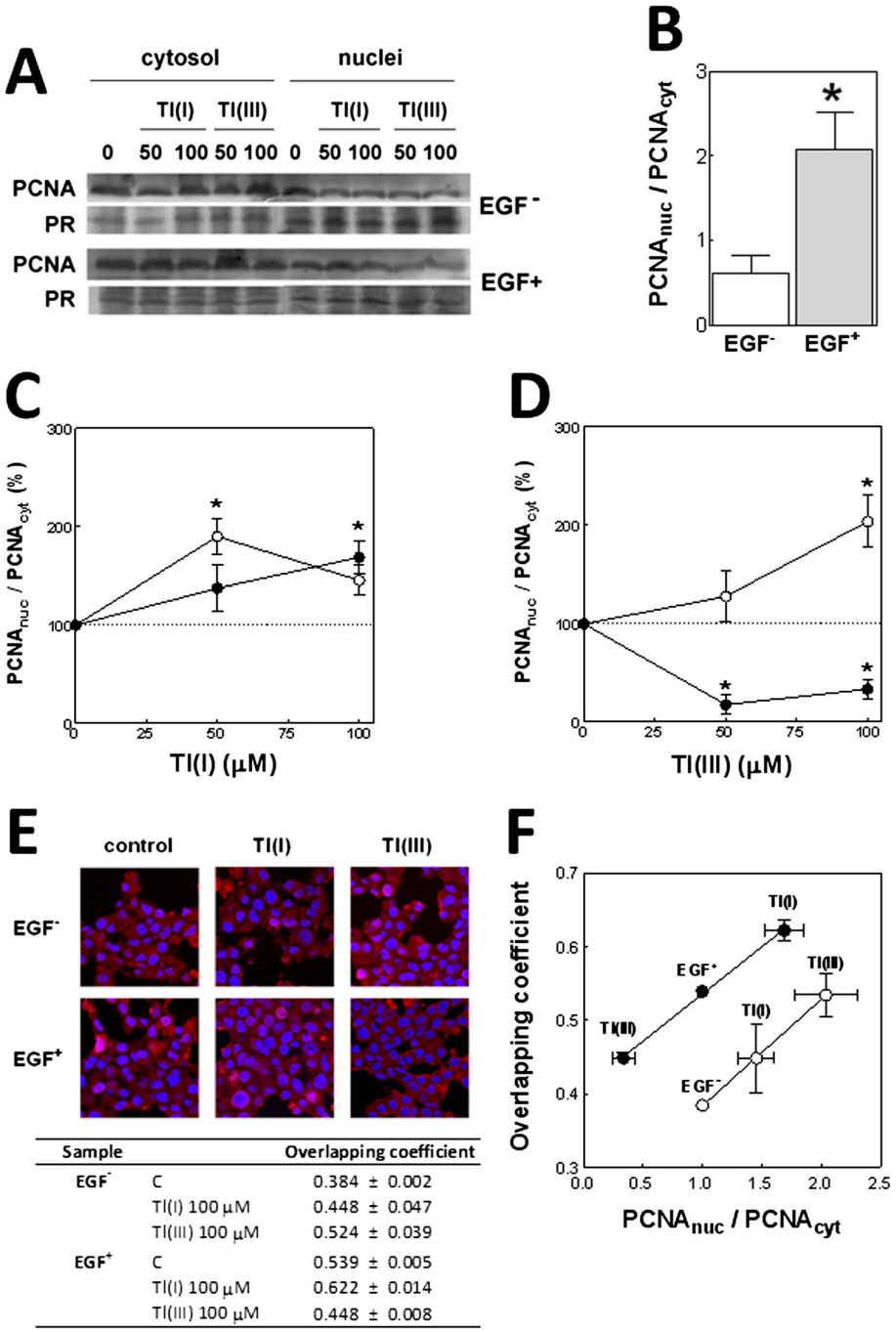

Sample		Overlapping coefficient
EGF⁻	C	0.384 ± 0.002
	Tl(I) 100 μM	0.448 ± 0.047
	Tl(III) 100 μM	0.524 ± 0.039
EGF⁺	C	0.539 ± 0.005
	Tl(I) 100 μM	0.622 ± 0.014
	Tl(III) 100 μM	0.448 ± 0.008

Figure 7. Effects of Tl on proliferating cell nuclear antigen (PCNA) localization. PC12 cells were incubated at 37 °C for 24 h in serum-free DMEM. After media replacement, EGF^- and EGF^+ cells were incubated for a further 24 h in the presence of 50 or 100 μM Tl(I) or Tl(III), and PCNA content was evaluated in nuclear and cytoplasmic fractions. (A) Representative Western blots. Loading control was performed by Ponceau Red (PR) protein staining and the region of the membrane corresponding to PCNA (36 kDa) migration is shown. (B) Nuclear ($PCNA_{nuc}$) to cytosolic ($PCNA_{cyt}$) PCNA ratio measured in EGF^- and EGF^+ cells. (C and D) Relative nuclear to cytosolic PCNA ratio measured in Tl(I)- and Tl(III)-treated cells, respectively. Results are shown as the mean ± SEM of at least three independent experiments. *Significantly different from the value measured in the corresponding fraction from cells incubated in the absence of Tl ($P < 0.01$). (E) PCNA immunolocalization in EGF^- (○) and EGF^+ (●) cells exposed for 24 h to 100 μM Tl(I) or Tl(III) and visualized by confocal microscopy. *Red*: PCNA; *blue*: nuclei. Table shows the overlapping coefficients calculated according to (Manders *et al.,* 1993). (F) Correlation between the overlapping coefficients calculated for PCNA immunolocalization and the relative nuclear to cytoplasmic PCNA levels measured in EGF^- and EGF^+ cells.

was chosen considering the maximal metal concentration found in Tl-poisoned people (Schaub, 1996). Based solely on cell DNA content measured at two fixed time points (24 and 30 h), it seems that Tl(I) and Tl(III) have different impacts on EGF^- cell-cycle progression. After 24 h, Tl(I) increased the amount of EGF^- cells in S phase, an effect that was accompanied by a decrease in the amount of cells in G_2/M. However, after 30 h, Tl(I)-treated cells had higher relative amounts of cells in the S and G_2/M

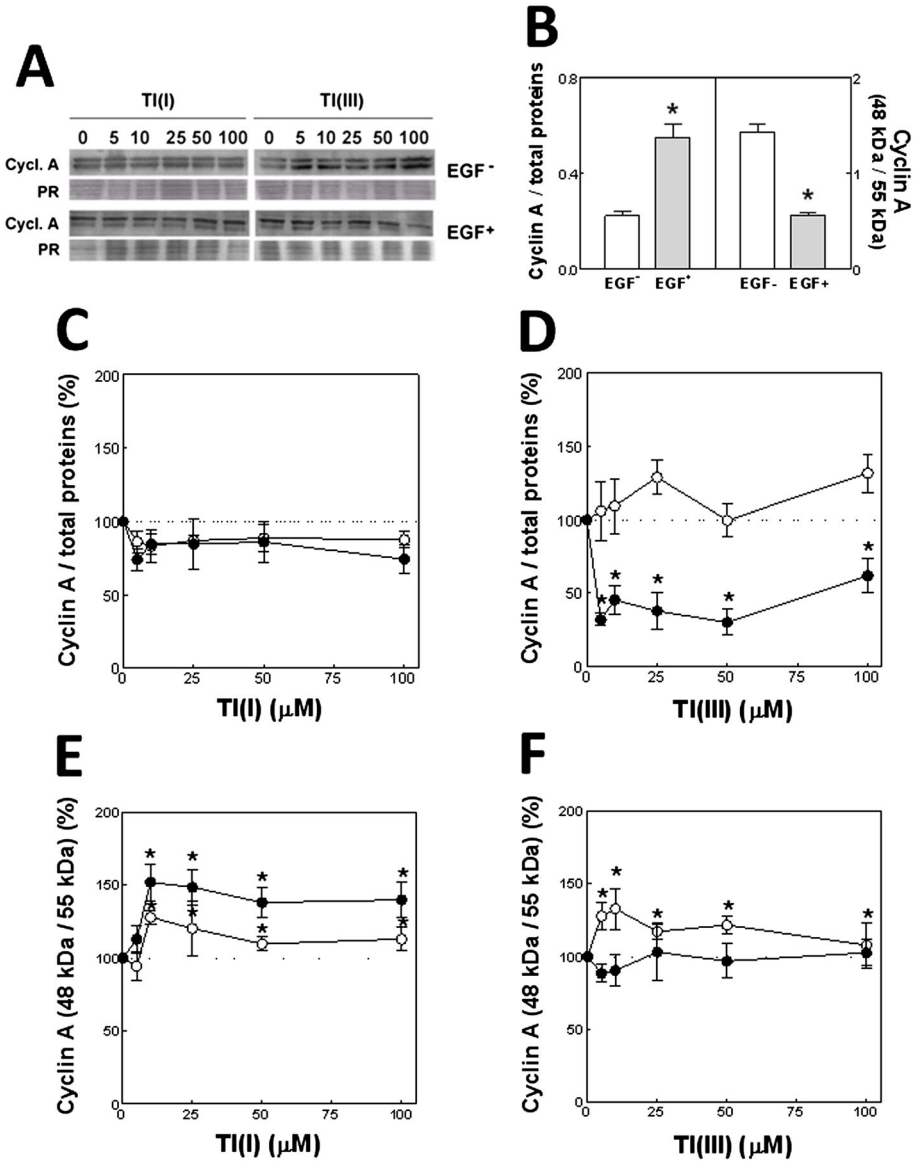

Figure 8. Effects of Tl on cyclin A expression. PC12 cells were incubated at 37 °C for 24 h in serum-free Dulbecco´s modified Eagle medium (DMEM). After media replacement, EGF^- and EGF^+ cells were incubated for a further 24 h in the presence of 5–100 μM Tl(I) or Tl(III), and cyclin A expression was evaluated. (A) Representative Western blots. Loading control was performed by Ponceau Red (PR) protein staining and the region of the membrane corresponding to cyclin A (55 kDa) migration is shown. (B) Total cyclin A content and cleaved (48 kDa) to full-length (55 kDa) cyclin A ratio in EGF^- (○) and EGF^+ (●) cells. (C and D) Total cyclin A contents in Tl(I)- and Tl(III)-treated cells, respectively. (E and F) Relative amount of cleaved (48 kDa) and full-length (55 kDa) cyclin A in Tl(I)- and Tl(III)-treated cells, respectively. Results are shown as the mean ± SEM of at least four independent experiments. * Significantly different from the value measured in cells incubated in the absence of Tl ($P < 0.01$).

phases, suggesting that Tl(I) may cause a mild delay in EGF^- cell-cycle resumption. Additionally, Tl(I) may cause EGF^- cell cycle arrest in G_2 similar to that observed in C6 glioma cells (Chia *et al.,* 2005). The exposure of those cells to 10–100 μM Tl(I) caused no major alterations in the cell cycle, although at higher concentrations, up to 3 mM, Tl(I) produced the arrest in the G_2 phase. In the current study, we did not investigate the effects of Tl(I) beyond the 100 μM concentration because of the large loss of cell viability that high concentrations of Tl(I) cause in PC12 cells (Hanzel and Verstraeten, 2006). In contrast to the observed for Tl(I), Tl(III) shortened the duration of G_1 in EGF^- cells. This conclusion is supported by the finding that at 24 h, Tl(III) increased the percentage of cells in G_2/M at the expense of decreasing the amount of cells in S whereas at 30 h, Tl(III) decreased the amount of cells in G_1 and increased the amount of those in S phase. Tl(I) and Tl(III) also displayed differential effects on the progression of the EGF^+ cell cycle. Tl(I) stimulated the resumption of cell entry into S phase, as observed both at 24 and 30 h of incubation. In contrast, Tl(III) delayed the entry on the S phase as suggested by the increased contents of cells in G_1 at 24 h followed by a decrease in the amount of cells in the S phase at 30 h of incubation. The effects of Tl(III) on the progression of cell cycle in any other cultured cell or animal models have not been reported yet, making this study a novel contribution to the knowledge of Tl(III) mechanisms of action in biological systems.

Journal of Applied Toxicology

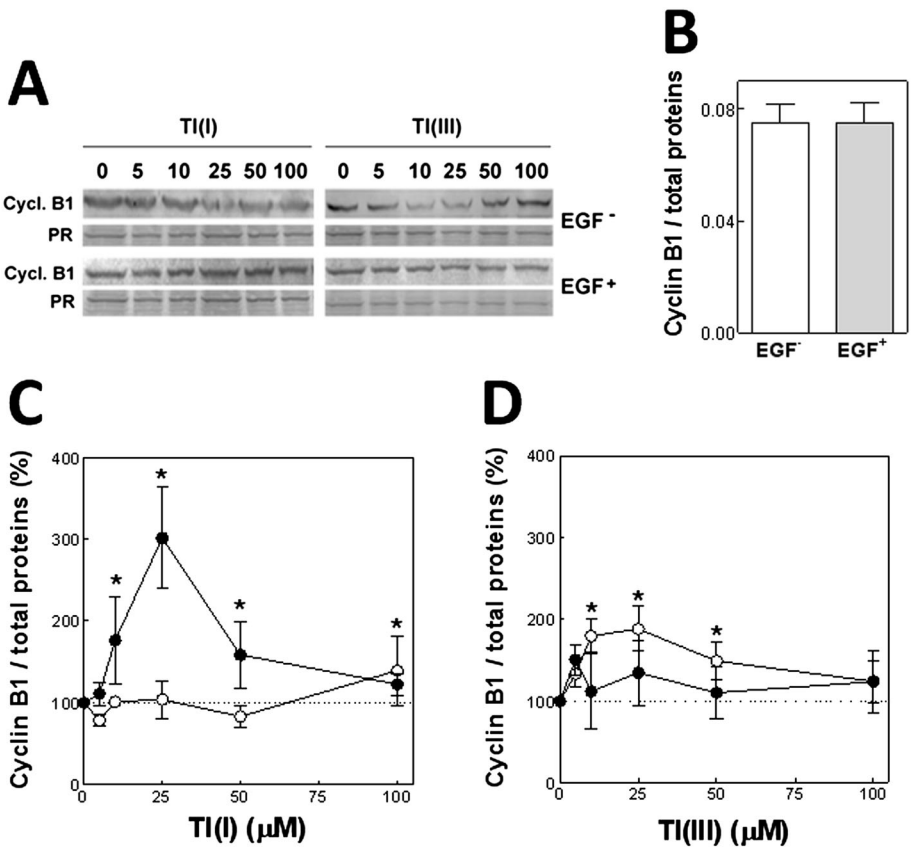

Figure 9. Effects of Tl on cyclin B1 expression. PC12 cells were incubated at 37 °C for 24 h in serum-free DMEM. After media replacement, EGF^- and EGF^+ cells were incubated for a further 24 h in the presence of 5–100 μM Tl(I) or Tl(III), and cyclin B1 expression was evaluated. (A) Representative Western blots. Loading control was performed by Ponceau Red (PR) protein staining and the region of the membrane corresponding to cyclin B1 (60 kDa) migration is shown. Graphs show the relative cyclin B1 content in EGF^- (○) and EGF^+ (●) cells (B), and in Tl(I)- (C) or Tl(III)-treated cells (D). Results are shown as the mean ± SEM of at least four independent experiments. * Significantly different from the value measured in cells incubated in the absence of Tl ($P < 0.01$).

The expression of the cyclin marker of each phase of the cycle was evaluated in whole samples and thus, the results obtained are the average of all cell populations. The fact that only a limited amount of cells entered the S phase constituted a valuable tool for our study, because the comparative analysis of the cyclins and other key regulators of cell-cycle progression allowed us to monitor simultaneously the status of each phase of the cycle.

EGF^- and EGF^+ cells expressed cyclin D1 to a similar extent. Through the activation of the retinoblastoma tumor suppressor protein (Rb), the cyclin D1-cdk4/6 complex regulates the expression of the E2F family of transcription factors. In turn, E2F-1 regulates cyclin E expression (Gopinathan *et al.,* 2011) and both, E2F-1 and cyclin E, control the $G_1 \rightarrow S$ transition. In non-proliferating cells, the cyclin D-cdk4/6 complex is bound, among others, to the inhibitory protein p21 located in the nucleus (Cmielova and Rezacova, 2011). Nuclear p21 also binds to cyclins E and A, and the proliferating cell nuclear antigen (PCNA), causing cell cycle arrest (Cazzalini *et al.,* 2010). Upon phosphorylation by Akt1, p21 exits the nuclei and the cycle proceeds to the S phase (Heron-Milhavet *et al.,* 2006). The higher content of p21 in the cytoplasm of EGF^+ cells, accompanied by the higher content of nuclear PCNA are indicative of cells in S phase. Supporting this, the expression of the S phase marker cyclin A, which is regulated by E2F-1 (Schulze *et al.,* 1995), was also increased in EGF^+ cells. Two bands corresponding to cyclin A were detected, the full-length protein (55 kDa) and a 48-kDa inactive fragment (Welm *et al.,* 2002). In EGF^+ cells, cyclin A expression was increased and its active form predominated. The expression of cyclin B1, that starts in late S phase and progressively increases until G_2 phase (Lindqvist *et al.,* 2009), was similar in EGF^- and EGF^+ cells. This finding is in accordance with the similar amounts of cells in G_2/M found in both experimental conditions.

Based on the pattern of expression of cyclins and cell-cycle regulators assessed, we can conclude that Tl(I) affected both G_1 and S phases of the EGF^- cell cycle. Tl(I) promoted the $G_1 \rightarrow S$ transition, as evidenced by the decrease in cyclin D1 and the increase in E2F-1 and cyclin E expression. Tl(I) also promoted the progression of S phase, as indicated by the exit of p21 from the nuclei and by the increased expression of nuclear PCNA and cyclin A. Regarding the $G_2 \rightarrow M$ transition, no major alterations were observed after 24 h, based on the levels of cyclin B1 that were consistent with the amount of cells in G_2/M. After 30 h of incubation, the amount of cells in G_2/M was markedly increased. This is an interesting finding because Tl(I) could alter chromosomal distribution and increase the number of cells with micronuclei, which leads to a decreased number of mitosis (Leonard and Gerber, 1997).

Tl(I) also stimulated G_1 and S phase progression in EGF^+ cells. In these cells, the markers of $G_1 \rightarrow S$ transition were increased,

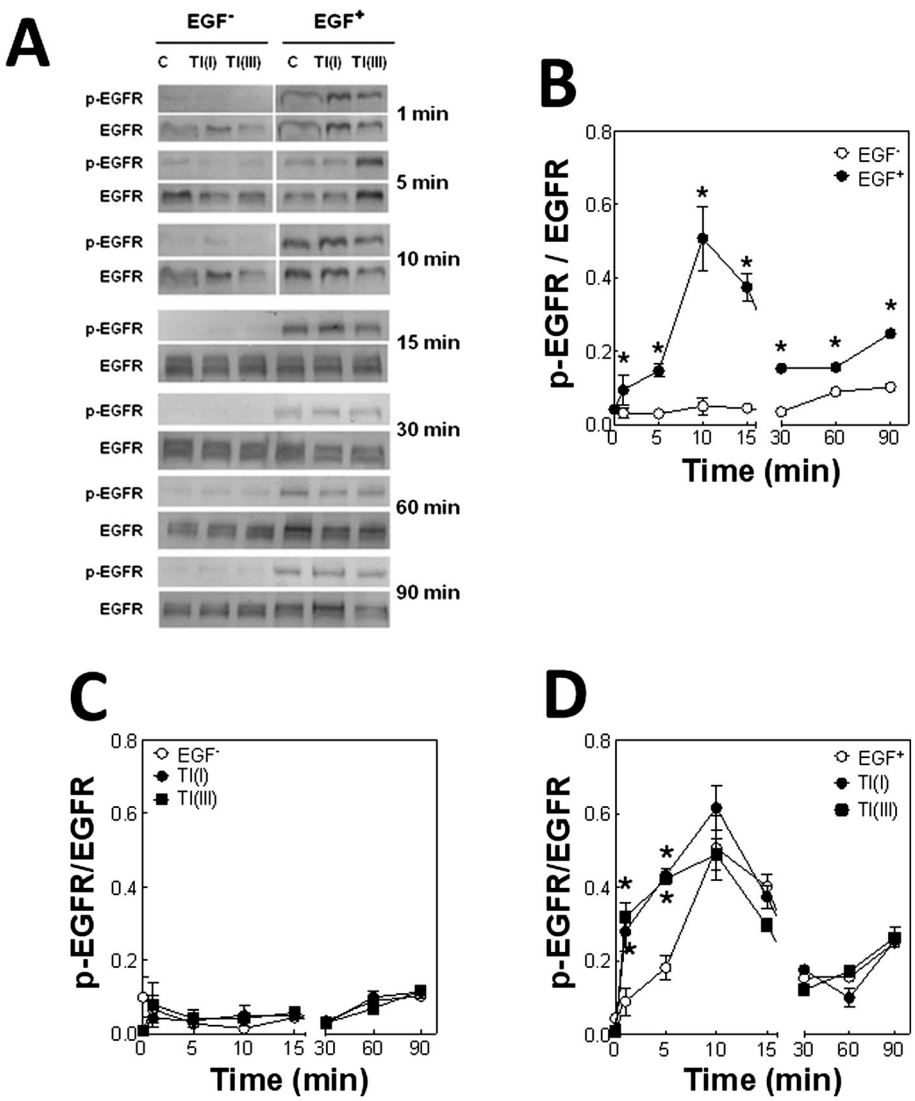

Figure 10. Effects of Tl on the kinetics of EGF receptor (EGFR) phosphorylation. PC12 cells were incubated at 37 °C for 24 h in serum-free Dulbecco´s modified Eagle medium (DMEM). After media replacement, EGF^- and EGF^+ cells were further incubated at 37 °C for 1–90 min in the absence of further additions (C) or in the presence of 100 μM Tl(I) or Tl(III), and the levels of phosphorylated EGFR (p-EGFR) and total EGFR were evaluated. (A) Representative Western blots. (B) Quantification of p-EGFR to total EGFR ratio in EGF^- (○) and EGF^+ (●) cells incubated in the absence of Tl. Results are shown as the mean ± SEM of four independent experiments. * Significantly different from the value measured in EGF^- cells at the same incubation time ($P < 0.01$). The ratio between p-EGFR to EGFR levels was determined in (C) EGF^- and (D) EGF^+ cells incubated in the absence of further additions (○) or in the presence of 100 μM Tl(I) (●) or Tl(III) (■). Results are shown as the mean ± SEM of four independent experiments. * Significantly different from the value measured in control EGF^+ cells at the same time point ($P < 0.05$).

suggesting that Tl(I) stimulated cell-cycle resumption. The mild effect on p21 and PCNA translocation, together with the finding that cyclin A was mostly inactive, suggests that at that time point (24 h) the S phase was concluding. In agreement with this, the analysis of DNA content showed an accumulation of cells in S phase. Finally, increased levels of cyclin B1 were found which stimulates the progression of G_2 towards mitosis. Supporting that, the amount of cells in G_2/M after 30 h was restored to control values, indicating the completion of the cycle.

Tl(III) had differential effects on the PC12 cell cycle. Tl(III) promoted $G_1 \rightarrow S$ transition in EGF^- cells, as suggested by the increased expression of E2F-1 and cyclin E. Even when Tl (III) induced the translocation of p21 and PCNA, the expression of cyclin A remained within control values with a mild increase in the amount of the inactive form. As discussed previously, these findings suggest that the progression of the S phase was accelerated. In line with this, Tl(III) affected positively the $G_2 \rightarrow M$ transition, as evidenced by the increase in cyclin B1 levels and the higher content of cells in G_2/M phase. Tl(III) did not affect EGF^- cell mitosis, as no further accumulation of cells in G_2/M was observed after 30 h, thus signifying that the cycle was completed. In contrast to the observed in EGF^- cells, Tl(III) postponed the resumption of the cycle in EGF^+ cells, as evidenced by the marked increase in cyclin D1 and by the decreased expression of E2F-1 and cyclin E. Furthermore, the levels of cyclin D1 after 24 h positively correlated with the amount of cells in G_0/G_1 phase. Moreover, the progression of the S phase was impaired, based on the higher p21 nuclear content with decreased expression of nuclear PCNA and total cyclin A. Importantly, this effect could not be

Journal of AppliedToxicology

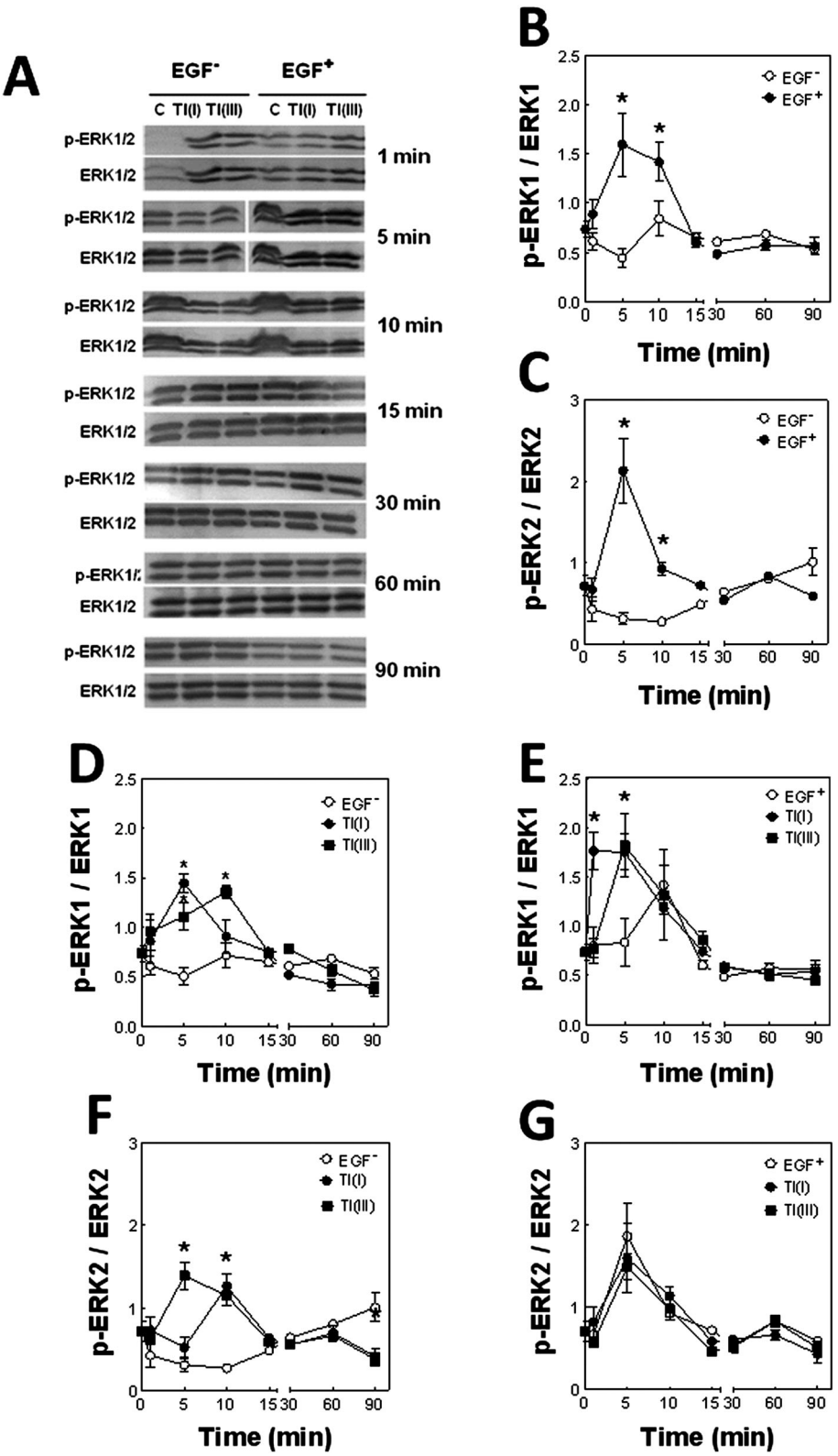

Figure 11. Effects of Tl on the kinetics of ERK1/2 phosphorylation. PC12 cells were incubated at 37 °C for 24 h in serum-free Dulbecco´s modified Eagle medium (DMEM). After media replacement, EGF^- and EGF^+ cells were further incubated at 37 °C for 1–90 min in the absence of further additions (C) or in the presence of 100 μM Tl(I) or Tl(III), and the levels of phosphorylated ERK1/2 (p-ERK1/2) and total ERK1/2 were evaluated. (A) Representative Western blots. (B and C) Quantification of p-ERK1 to ERK1 (B) and p-ERK2 to ERK2 (C) ratios in EGF^- (○) and EGF^+ (●) cells incubated in the absence of Tl. (D–G) Quantification of p-ERK1 to ERK1 ratio (D and E) and p-ERK2 to ERK2 ratio (F and G) measured in EGF^- (D, F) and EGF^+ (E, G) cells incubated in the absence of further additions (○) or in the presence of 100 μM Tl(I) (●) or Tl(III) (■). Results are shown as the mean ± SEM of four independent experiments. * Significantly different from the value measured in cells incubated in the absence of Tl ($P < 0.01$).

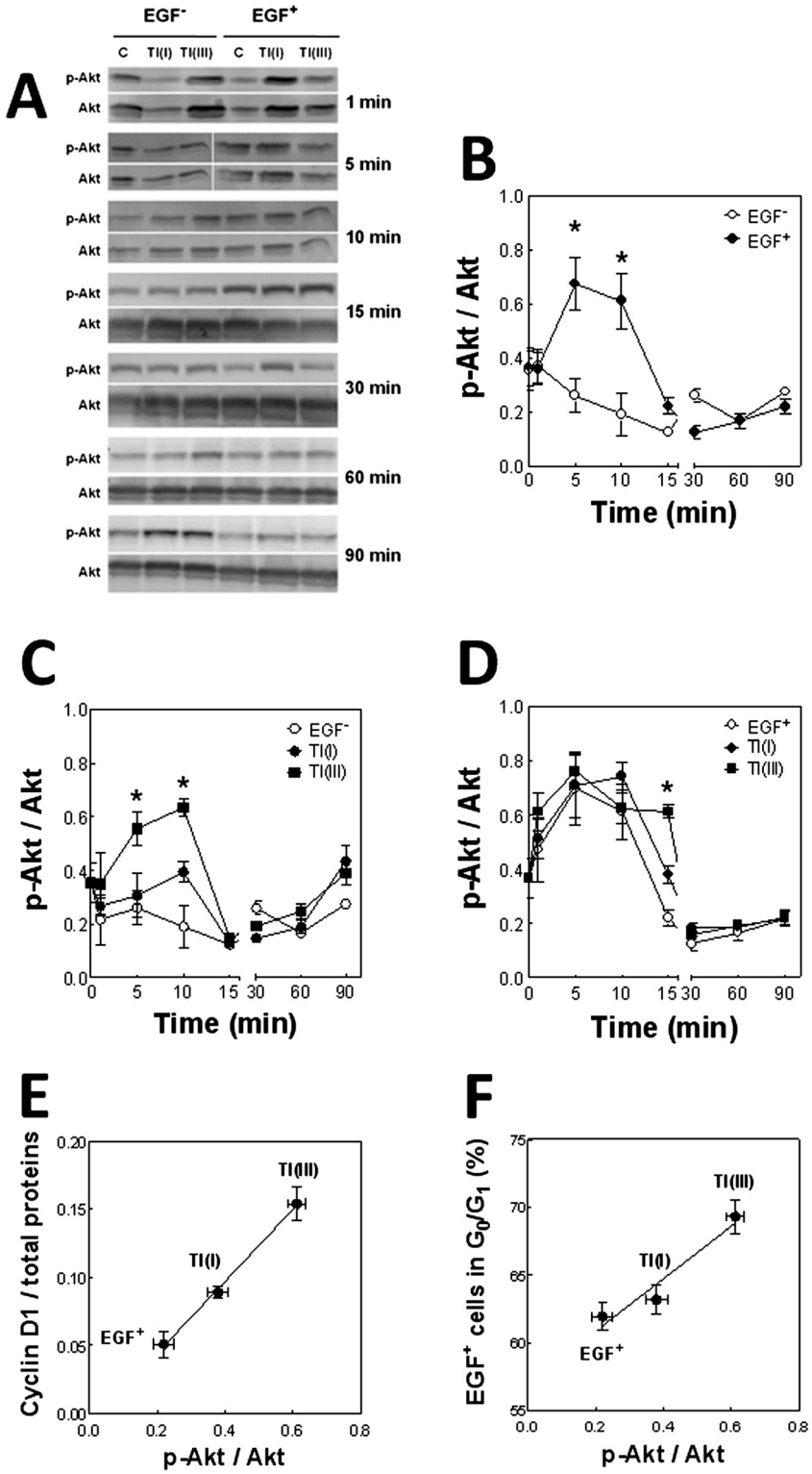

Figure 12. Effects of Tl on the kinetics of Akt phosphorylation. PC12 cells were incubated at 37 °C for 24 h in serum-free Dulbecco´s modified Eagle medium (DMEM). After media replacement, EGF^- and EGF^+ cells were further incubated at 37 °C for 1–90 min in the absence of further additions (C) or in the presence of 100 μM Tl(I) or Tl(III), and the levels of phosphorylated Akt (p-Akt) and total Akt were evaluated. (A) Representative Western blots. (B) Quantification of p-Akt to total Akt ratio in EGF^- (○) and EGF^+ (●) cells incubated in the absence of Tl. Results are shown as the mean ± SEM of four independent experiments. * Significantly different from the value measured in EGF^- cells at the same incubation time ($P < 0.01$). The ratio between p-Akt and Akt levels was determined in (C) EGF^- and (D) EGF^+ cells incubated in the absence of further additions (●) or in the presence of 100 μM Tl(I) (●) or Tl(III) (■). Results are shown as the mean ± SEM of four independent experiments. * Significantly different from the value measured in cells incubated in the absence of Tl ($P < 0.01$). (E) Correlation between Akt phosphorylation in EGF^+ cells exposed for 15 min to 100 μM Tl(I) or Tl(III) and cyclin D1 expression levels. (F) Correlation between Akt phosphorylation in EGF^+ cells exposed for 15 min to 100 μM Tl(I) or Tl(III) and the amount of cells in the G_0/G_1 phase.

ascribed to a Tl(III)-mediated oxidation of EGF that would limit its interaction with the EGFR.

To characterize further the mechanisms underlying Tl(I)- and Tl(III)-mediated alterations in the progression of EGF^- and EGF^+ cell cycle, the kinetics of the initial steps of EGF-dependent signaling cascade were next evaluated. Both Tl(I) and Tl(III) (100 μM) enhanced EGF-dependent phosphorylation of EGFR within 1 and 5 min of incubation, while at prolonged incubations the extent of EGFR phosphorylation was similar to that caused by EGF alone. The finding that EGFR activation was enhanced by Tl after only 1 min of incubation was unexpected. At this time point, neither Tl(I) nor Tl(III) could enter cells to a significant amount, implying that this effect must take place at the extracellular side of the plasma membrane. One plausible explanation involves the activation of the voltage-gated calcium channels (VGCC). The opening of these channels is triggered by the depolarization of the plasma membrane and causes a rapid rise in cytoplasmic Ca^{2+} concentration, which in turn induces EGFR phosphorylation (Zwick *et al.,* 1999). We demonstrated previously that the interaction of Tl(I) and Tl(III) with lipid bilayers induced a rapid increase in the membrane surface potential (Villaverde and Verstraeten, 2003) that, in case of occurring in biological membranes, may result in the depolarization of the plasma membrane. The possibility that this mechanism may be operative in our experimental model is currently under investigation.

EGF induces ERK1/2 (Mebratu and Tesfaigzi, 2009) and Akt (Manning and Cantley, 2007) phosphorylation, which are associated with cell survival and proliferation. Tl(I) and Tl(III) induced the phosphorylation of ERK1 and ERK2 in EGF^- cells, whereas they affected only ERK1 phosphorylation in EGF^+ cells. The molecular mechanisms underlying the differential activation of ERK1 and ERK2 remain to be elucidated. The kinetics of Tl(I)- and Tl(III)-mediated ERK1, ERK2 and Akt phosphorylation in EGF^- cells resembled those caused by EGF alone, suggesting that they may mimic the effects of EGF even in the absence of EGFR activation. Conversely, these cations may enhance in EGF^- cells the activation of RTKs by other growth factors present in the culture media, an effect that could be masked upon EGF supplementation. In Tl(I)- and Tl(III)-treated EGF^+ cells, Akt was still activated after 15 min of incubation and this effect correlated positively with the amount of cells in G_0/G_1 and the expression of cyclin D1. As Akt regulates the expression and phosphorylation of p21 and stabilizes cyclin D (Liang and Slingerland, 2003; Hassan *et al.,* 2013), these findings imply that Tl-mediated ERK1/2 and Akt phosphorylation are key in the resumption of the cell cycle both in EGF^- and EGF^+ cells.

Altogether, experimental evidence presented in this work indicate that Tl(I) and Tl(III) have dissimilar effects on PC12 cells proliferation, and that those effects depended not only on the concentration of the metal in the media but also on cell stimulation with a growth factor, e.g. EGF. In agreement with our previous findings, the effects due to Tl(I) were different in magnitude and/or kinetics than those due to Tl(III) (Hanzel and Verstraeten, 2006; Hanzel and Verstraeten, 2009; Hanzel *et al.,* 2012), thus supporting the hypothesis that Tl(III)-mediated effects on cell outcome are caused by Tl(III) itself, and not by Tl(I) generated from the reduction of Tl(III) in the extracellular milieu. The finding that neither Tl(I) nor Tl(III) abolished cell proliferation in this cell model, and that EGF partially prevented cell apoptosis induced by these cations (Pino & Verstraeten, unpublished results) helps to understand why in non-fatal cases of Tl poisoning, most clinical symptoms can be ameliorated (Cvjetko *et al.,* 2010). The capacity to restore the affected functions seems to rely on the intrinsic ability of organs and tissues to proliferate and regenerate the affected areas, which is altered but not fully impaired by Tl. In line with this, being the peripheral nerves able to regenerate and to reinervate the denervated targets (Fu and Gordon, 1997), the sensory and motor alterations caused by Tl exposure can be fully reverted. In this system, the release of neurotrophic and growth factors, including EGF, by cells in the surroundings of the lesion induces neuronal regeneration (Fu and Gordon, 1997). In contrast, the alterations of the central nervous system, such as the optic atrophy responsible for the generation of central scotoma (Schmidt *et al.,* 1997), persist even after the normalization of Tl content in the body fluids. In this case, the lack of tissular regeneration cannot be ascribed to the toxic effects of Tl but to the extremely low or no neuronal regeneration in the central nervous system.

Acknowledgments

This work was supported by grants of the University of Buenos Aires (B086 and 20020100100112); Consejo Nacional de Investigación Científica y Tecnológica (CONICET) (PIP 112-200801-01977); and Agencia Nacional de Promoción Científica y Tecnológica (ANPCyT) (PICT 32273), Argentina. SVV is a career investigator of the CONICET (National Research Council, Argentina). Authors are grateful to Dr Ana M Adamo, Dr Leonor Roguin and Dr Lorena Gonzalez for the generous gift of the antibodies against PCNA, ERK1/2 and EGFR, respectively.

Conflict of Interest

The Authors did not report any conflict of interest.

References

Anchan RM, Reh TA, Angello J, Balliet A, Walker M. 1991. EGF and TGF-alpha stimulate retinal neuroepithelial cell proliferation in vitro. *Neuron* **6**: 923–936.

ATSDR. 1999. Thallium. ATSDR (Agency for Toxic Substances and Disease Registry). Prepared by Clement International Corp., under contract 205-88-0608: Atlanta, GA

Birk D, Gansauge F, Gansauge S, Formentini A, Lucht A, Beger HG. 1999. Serum and correspondent tissue measurements of epidermal growth factor (EGF) and epidermal growth factor receptor (EGF-R). Clinical relevance in pancreatic cancer and chronic pancreatitis. *Int. J. Pancreatol.* **25**: 89–96.

Bose R, Onishchenko N, Edoff K, Janson Lang AM, Ceccatelli S. 2012. Inherited effects of low-dose exposure to methylmercury in neural stem cells. *Toxicol. Sci.* **130**: 383–390.

Bradford MM. 1976. A rapid and sensitive method for the quantitation of microgram quantities of protein utilizing the principle of protein-dye binding. *Anal. Biochem.* **72**: 248–254.

Bunzl K, Trautmannsheimer M, Schramel P, Reifenhäuser W. 2001. Availability of arsenic, copper, lead, thallium, and zinc to various vegetables grown in slag-contaminated soils. *J. Environ. Qual.* **30**: 934–939.

Cazzalini O, Scovassi AI, Savio M, Stivala LA, Prosperi E. 2010. Multiple roles of the cell cycle inhibitor p21(CDKN1A) in the DNA damage response. *Mutat. Res.* **704**: 12–20.

Cmielova J, Rezacova M. 2011. p21Cip1/Waf1 protein and its function based on a subcellular localization [corrected]. *J. Cell. Biochem.* **112**: 3502–3506.

Cooper S. 2000. The continuum model and G1-control of the mammalian cell cycle. *Prog. Cell Cycle Res.* **4**: 27–39.

Cooper S. 2003. Reappraisal of serum starvation, the restriction point, G0, and G1 phase arrest points. *FASEB J.* **17**: 333–340.

Cvjetko P, Cvjetko I, Pavlica M. 2010. Thallium toxicity in humans. *Arh. Hig. Rada Toksikol.* **61**: 111–119.

Cheam V. 2001. Thallium contamination of water in Canada. *Water Qual. Res. J. Canada* **36**: 851–877.

Chia CF, Chen SC, Chen CS, Shih CM, Lee HM, Wu CH. 2005. Thallium acetate induces C6 glioma cell apoptosis. *Ann. N. Y. Acad. Sci.* **1042**: 523–530.

Darolles C, Sage N, Armengaud J, Malard V. 2013. In vitro assessment of cobalt oxide particle toxicity: identifying and circumventing interference. *Toxicol. In Vitro* **27**: 1699–1710.

Fu SY, Gordon T. 1997. The cellular and molecular basis of peripheral nerve regeneration. *Mol. Neurobiol.* **14**: 67–116.

Fujita K, Lazarovici P, Guroff G. 1989. Regulation of the differentiation of PC12 pheochromocytoma cells. *Environ. Health Perspect.* **80**: 127–142.

Galvan-Arzate S, Santamaria A. 1998. Thallium toxicity. *Toxicol. Lett.* **99**: 1–13.

Gastaldo J, Viau M, Bencokova Z, Joubert A, Charvet AM, Balosso J, Foray N. 2007. Lead contamination results in late and slowly repairable DNA double-strand breaks and impacts upon the ATM-dependent signaling pathways. *Toxicol. Lett.* **173**: 201–214.

Glahn F, Schmidt-Heck W, Zellmer S, Guthke R, Wiese J, Golka K, Hergenroder R, Degen GH, Lehmann T, Hermes M, Schormann W, Brulport M, Bauer A, Bedawy E, Gebhardt R, Hengstler JG, Foth H. 2008. Cadmium, cobalt and lead cause stress response, cell cycle deregulation and increased steroid as well as xenobiotic metabolism in primary normal human bronchial epithelial cells which is coordinated by at least nine transcription factors. *Arch. Toxicol.* **82**: 513–524.

Gopinathan L, Ratnacaram C, Kaldis P. 2011. Established and Novel Cdk/Cyclin Complexes Regulating the Cell Cycle and Development. In *Cell Cycle in Development*, Kubiak JZ (ed). Springer: Berlin; 365–389

Greene LA, Tischler AS. 1976. Establishment of a noradrenergic clonal line of rat adrenal pheochromocytoma cells which respond to nerve growth factor. *Proc. Natl. Acad. Sci. U. S. A.* **73**: 2424–2428.

Hanzel CE, Almeira Gubiani MF, Verstraeten SV. 2012. Endosomes and lysosomes are involved in early steps of Tl(III)-mediated apoptosis in rat pheochromocytoma (PC12) cells. *Arch. Toxicol.* **86**: 1667–1680.

Hanzel CE, Verstraeten SV. 2006. Thallium induces hydrogen peroxide generation by impairing mitochondrial function. *Toxicol. Appl. Pharmacol.* **216**: 485–492.

Hanzel CE, Verstraeten SV. 2009. Tl(I) and Tl(III) activate both mitochondrial and extrinsic pathways of apoptosis in rat pheochromocytoma (PC12) cells. *Toxicol. Appl. Pharmacol.* **236**: 59–70.

Hassan B, Akcakanat A, Holder AM, Meric-Bernstam F. 2013. Targeting the PI3-kinase/Akt/mTOR signaling pathway. *Surg. Oncol. Clin. N. Am.* **22**: 641–664.

Heim M, Wappelhorst O, Markert B. 2002. Thallium in terrestrial environments - Occurrence and effects. *Ecotoxicology* **11**: 369–377.

Henson ES, Gibson SB. 2006. Surviving cell death through epidermal growth factor (EGF) signal transduction pathways: implications for cancer therapy. *Cell. Signal.* **18**: 2089–2097.

Heron-Milhavet L, Franckhauser C, Rana V, Berthenet C, Fisher D, Hemmings BA, Fernandez A, Lamb NJ. 2006. Only Akt1 is required for proliferation, while Akt2 promotes cell cycle exit through p21 binding. *Mol. Cell Biol.* **26**: 8267–8280.

Hoffman RS. 2000. Thallium poisoning during pregnancy: a case report and comprehensive literature review. *J. Toxicol. Clin. Toxicol.* **38**: 767–775.

Hwang DL, Lev-Ran A, Tay YC, Chen CR, Dev N. 1989. Epidermal growth factor excretion and receptor binding in diabetic rats. *Life Sci.* **44**: 407–416.

Joh T, Itoh M, Katsumi K, Yokoyama Y, Takeuchi T, Kato T, Wada Y, Tanaka R. 1986. Physiological concentrations of human epidermal growth factor in biological fluids: use of a sensitive enzyme immunoassay. *Clin. Chim. Acta* **158**: 81–90.

Krasnodebska-Ostrega B, Sadowska M, Ostrowska S. 2012. Thallium speciation in plant tissues-Tl(III) found in Sinapis alba L. grown in soil polluted with tailing sediment containing thallium minerals. *Talanta* **93**: 326–329.

Law S, Turner A. 2011. Thallium in the hydrosphere of south west England. *Environ. Pollut.* **159**: 3484–3489.

Lee SD, Lo MJ. 2010. Ginsenoside Rb1 promotes PC12 cell cycle kinetics through an adenylate cyclase-dependent protein kinase A pathway. *Nutr. Res.* **30**: 660–666.

Leonard A, Gerber GB. 1997. Mutagenicity, carcinogenicity and teratogenicity of thallium compounds. *Mutat. Res.* **387**: 47–53.

Liang J, Slingerland JM. 2003. Multiple roles of the PI3K/PKB (Akt) pathway in cell cycle progression. *Cell Cycle* **2**: 339–345.

Lindqvist A, Rodriguez-Bravo V, Medema RH. 2009. The decision to enter mitosis: feedback and redundancy in the mitotic entry network. *J. Cell Biol.* **185**: 193–202.

Mahanthappa NK, Schwarting GA. 1993. Peptide growth factor control of olfactory neurogenesis and neuron survival in vitro: roles of EGF and TGF-beta s. *Neuron* **10**: 293–305.

Manders EMM, Verbeek FJ, Aten JA. 1993. Measurement of co-localization of objects in dual-colour confocal images. *J. Microsc.* **169**: 375–382.

Manning BD, Cantley LC. 2007. AKT/PKB signaling: navigating downstream. *Cell* **129**: 1261–1274.

Mebratu Y, Tesfaigzi Y. 2009. How ERK1/2 activation controls cell proliferation and cell death: Is subcellular localization the answer? *Cell Cycle* **8**: 1168–1175.

Mouri K, Sako Y. 2013. Optimality conditions for cell-fate heterogeneity that maximize the effects of growth factors in PC12 cells. *PLoS Comput. Biol.* **9**: e1003320.

Muller JM, Rupec RA, Baeuerle PA. 1997. Study of gene regulation by NF-kappa B and AP-1 in response to reactive oxygen intermediates. *Methods* **11**: 301–312.

Mytilineou C, Park TH, Shen J. 1992. Epidermal growth factor-induced survival and proliferation of neuronal precursor cells from embryonic rat mesencephalon. *Neurosci. Lett.* **135**: 62–66.

Nikiforov A, Slozina N, Neronova E, Kharchenko T, Sosukin A, Scherbak S, Sarana A, Onikienko S. 1999. Cytogenetic investigation of thallium-poisoned people: pilot study. *J. Toxicol. Environ. Health A* **58**: 465–468.

Pavlickova J, Zbiral J, Smatanova M, Habarta P, Houserova P, Kuban V. 2006. Uptake of thallium from naturally-contaminated soils into vegetables. *Food Addit. Contam.* **23**: 484–491.

Peter AL, Viraraghavan T. 2005. Thallium: a review of public health and environmental concerns. *Environ. Int.* **31**: 493–501.

Queirolo F, Stegen S, Contreras-Ortega C, Ostapczuk P, Queirolo A, Paredes B. 2009. Thallium levels and bioaccumulation in environmental samples of northern Chile: human health risks. *J. Chil. Chem. Soc.* **54**: 464–469.

Repetto G, Del Peso A, Repetto M. 1998. Human thallium toxicity. In *Thallium in the environment. Advances in Environmental Science and Technology*, Nriagu J (ed). Wiley: New York, USA; 167–199

Reynolds BA, Tetzlaff W, Weiss S. 1992. A multipotent EGF-responsive striatal embryonic progenitor cell produces neurons and astrocytes. *J. Neurosci.* **12**: 4565–4574.

Rodriguez-Mercado JJ, Altamirano-Lozano MA. 2013. Genetic toxicology of thallium: a review. *Drug Chem. Toxicol.* **36**: 369–383.

Ronchetti SA, Miler EA, Duvilanski BH, Cabilla JP. 2013. Cadmium mimics estrogen-driven cell proliferation and prolactin secretion from anterior pituitary cells. *PLoS One* **8**: e81101.

Rudkin BB, Lazarovici P, Levi BZ, Abe Y, Fujita K, Guroff G. 1989. Cell cycle-specific action of nerve growth factor in PC12 cells: differentiation without proliferation. *EMBO J.* **8**: 3319–3325.

Sabbioni E, Marafante E, Rade J, Di Nucci A, Gregotti C, Manzo L. 1981. Metabolic patterns of low and toxic doses of thallium in the rat. In *Mechanisms of Toxicity and Hazard Evaluation*, Holmstedt B, Lauwerys R, Mercier M, Roberfroid M (eds). Elsevier: North-Holland; 559–564

Santa-Olalla J, Covarrubias L. 1995. Epidermal growth factor (EGF), transforming growth factor-alpha (TGF-alpha), and basic fibroblast growth factor (bFGF) differentially influence neural precursor cells of mouse embryonic mesencephalon. *J. Neurosci. Res.* **42**: 172–183.

Schaub G. 1996. Effects on humans. In *Thallium*, Schaub G (ed). World Health Organization: Geneva; 147–168

Schmidt D, Bach M, Gerling J. 1997. A case of localized retinal damage in thallium poisoning. *Int. Ophthalmol.* **21**: 143–147.

Schulze A, Zerfass K, Spitkovsky D, Middendorp S, Bergès J, Helin K, Jansen-Dürr P, Henglein B. 1995. Cell cycle regulation of the cyclin A gene promoter is mediated by a variant E2F site. *Proc. Natl. Acad. Sci. U. S. A.* **92**: 11264–11268.

Seroogy KB, Gall CM, Lee DC, Kornblum HI. 1995. Proliferative zones of postnatal rat brain express epidermal growth factor receptor mRNA. *Brain Res.* **670**: 157–164.

Simoniello P, Trinchella F, Filosa S, Scudiero R, Magnani D, Theil T, Motta CM. 2014. Cadmium contaminated soil affects retinogenesis in lizard embryos. *J. Exp. Zool. A Ecol. Genet. Physiol.* **321**: 207–219.

Smith LJ, Holmes AL, Kandpal SK, Mason MD, Zheng T, Wise JP Sr. 2014. The cytotoxicity and genotoxicity of soluble and particulate cobalt in human lung fibroblast cells. *Toxicol. Appl. Pharmacol.* **278**: 259–265.

Suresh Babu CV, Yoon S, Nam HS, Yoo YS. 2004. Simulation and sensitivity analysis of phosphorylation of EGFR signal transduction pathway in PC12 cell model. *Syst. Biol. (Stevenage)* **1**: 213–221.

Traverse S, Gomez N, Paterson H, Marshall C, Cohen P. 1992. Sustained activation of the mitogen-activated protein (MAP) kinase cascade may be required for differentiation of PC12 cells. Comparison of the effects of nerve growth factor and epidermal growth factor. *Biochem. J.* **288**(Pt 2): 351–355.

Traverse S, Seedorf K, Paterson H, Marshall CJ, Cohen P, Ullrich A. 1994. EGF triggers neuronal differentiation of PC12 cells that overexpress the EGF receptor. *Curr. Biol.* **4**: 694–701.

Villaverde MS, Verstraeten SV. 2003. Effects of thallium(I) and thallium(III) on liposome membrane physical properties. *Arch. Biochem. Biophys.* **417**: 235–243.

Welm AL, Timchenko NA, Ono Y, Sorimachi H, Radomska HS, Tenen DG, Lekstrom-Himes J, Darlington GJ. 2002. C/EBPα Is Required for Proteolytic Cleavage of Cyclin A by Calpain 3 in Myeloid Precursor Cells. *J. Biol. Chem.* **277**: 33848–33856.

Wierzbicka M, Szarek-Lukaszewska G, Grodzinska K. 2004. Highly toxic thallium in plants from the vicinity of Olkusz (Poland). *Ecotoxicol. Environ. Saf.* **59**: 84–88.

Xiao T, Guha J, Boyle D, Liu CQ, Chen J. 2004. Environmental concerns related to high thallium levels in soils and thallium uptake by plants in southwest Guizhou. *China. Sci. Total Environ.* **318**: 223–244.

Yamada M, Ikeuchi T, Hatanaka H. 1997. The neurotrophic action and signalling of epidermal growth factor. *Prog. Neurobiol.* **51**: 19–37.

Zhou Z, Wang C, Liu H, Huang Q, Wang M, Lei Y. 2013. Cadmium induced cell apoptosis, DNA damage, decreased DNA repair capacity, and genomic instability during malignant transformation of human bronchial epithelial cells. *Int. J. Med. Sci.* **10**: 1485–1496.

Zwick E, Wallasch C, Daub H, Ullrich A. 1999. Distinct calcium-dependent pathways of epidermal growth factor receptor transactivation and PYK2 tyrosine phosphorylation in PC12 cells. *J. Biol. Chem.* **274**: 20989–20996.

SUPPORTING INFORMATION

Additional supporting information may be found in the online version of this article at the publisher's web-site.